

University of Naples Federico II



Department of Pharmacy

Ph.D. in Pharmaceutical Science

XXVI° cycle

“Development of new self-assembling nanoparticles for the delivery of active agents for the treatment of tumors”

Ph.D. Course Coordinator

Prof. Maria Valeria D’Auria

Ph.D. Candidate

Giuseppina Salzano

Advisor

Prof. Giuseppe De Rosa

Indice

Introduction	1
Objective	6
Chapter 1	
Summary	8
Introduction.....	10
Materials.....	13
Materials and methods	13
Preparation of self-assembled NPs encapsulating ZOL	13
Preparation of self-assembled NPs encapsulating ZOL functionalized with human Transferrin.....	15
Characterization of PLCaPZ NPs and Tf-PLCaPZ NPs.....	15
Hemolysis assay	16
Cell lines, protein extraction and western blotting	17
Analysis of NPs intracellular distribution by FACS and confocal microscopy	18
Confocal Microscopy Analysis of Double Immunofluorescence.....	19
Cell proliferation by MTT assay	20
Drug combination studies	20
<i>In vivo</i> : Therapeutic efficacy in an heterotopic and orthotopic model s of GBM.....	21
Cell line	21
<i>In vivo</i> experiments	21
Bioluminescence imaging analysis	23
Statistical analysis	24
Results	25
Expression of Tf receptor in GBM cells and cytotoxicity studies.....	26
Tf-PLCaPZ NPs uptake and intracellular distribution.....	29
Effects of Tf-PLCaPZ NPs on the differentiation of GBM cells.....	31
Anti-proliferative effects of the sequential administration of Tf-PLCaPZ NPs and TMZ on GBM cells.	33
Antitumor efficacy of Tf-PLCaPZ NPs in heterotopic model of GBM .	35
Antitumor efficacy of Tf-PLCaPZ NPs in an orthotopic model of GBM	37
Discussion	39
Conclusions	44
Chapter 2	45
Summary	45
Introduction.....	47

Materials and Methods.....	52
Materials.....	52
Cell Culture.....	53
Synthesis of survivin siRNA-S-S-PE Conjugate.....	54
Incorporation of siRNA-S-S-PE in PEG2000-PE Micelles.....	54
Preparation and characterization of multifunctional PM co-encapsulating survivin siRNA and PXL.....	55
Characterization of PM.....	55
Incorporation of siRNA-S-S-PE Conjugate in PEG2000-PE PM.....	56
Cell viability assay.....	56
Chemosensitization Study.....	57
Survivin Protein Assay.....	57
Immunohistochemical staining.....	58
In vitro cytotoxicity of PM co-loaded with the combination of survivin siRNA-S-S-PE and PXL.....	59
<i>In vivo</i> studies: Cell Culture.....	59
Experimental model.....	60
Subcutaneous tumor xenografts development.....	60
Evaluation of therapeutic efficacy.....	61
Evaluation of repeated dose toxicity in mice.....	61
Evaluation of survivin mRNA expression by using RT-PCR.....	62
Collection of Tumor Tissues.....	62
Tumor cell apoptosis.....	62
Determination of survivin protein expression by immunofluorescence analysis.....	63
Evaluation of the simultaneous intra-tumor accumulation of PXL and down-regulation of survivin expression in tumor sections.....	64
Tubulin immunostaining.....	64
Statistical analysis.....	65
Results.....	66
Synthesis and characterization of survivin siRNA PM.....	66
Effect of survivin siRNA PM on the viability of cancer cell lines.....	68
Survivin protein levels.....	69
Chemosensitization study.....	70
Multifunctional therapy: survivin siRNA-S-S-PE and PXL co- encapsulated in PM.....	73
Therapeutic efficacy of survivin siRNA/PXL PM on an animal model of PXL resistant ovarian cancer, SKOV3-tr.....	74
Tumor tissues apoptosis.....	78

Down-regulation of survivin mRNA expression <i>in vivo</i>	78
Espression of survivin protein detected by immunofluorescence analysis	80
Effect of survivin siRNA/PXL PM on microtubule conformation of ovarian cancer xenografts	83
Discussion	85
Conclusions	92
References	I

Introduction

Therapeutic approaches for cancer treatment have been evolving while still struggling with several limitations. Non-specificity is the underlying reason for unwanted effects of chemotherapeutic agents on normal cells (Grivennikov S., 2010). One of the main downside is the multi-drug resistance (MDR) of cancer cells to chemotherapeutic agents (Xue X. *et al.*, 2012). Chemo-resistance is a multifactorial process directly linked to an over-expression or suppression of certain molecular pathways with consequent treatment failure. Currently applied strategies to manage chemo-resistant cancers in clinical oncology involve re-challenging the disease with novel formulations of conventional chemotherapeutics. In some cases, the development of formulations able to change the drug distribution and to increase drug accumulation into the tumor tissue/cells can allow to re-consider “old drugs” that can be transformed in new and powerful anticancer agents (De Rosa G. *et al.*, 2013). Furthermore, the combination of chemotherapeutics and agents with selective knockdown of genes responsible for altering the susceptibility of these drugs, such as small interfering RNA (siRNA), may lead to a synergistic effect in response to the treatments. However, the very rapid degradation of the nucleic acids in biological environment, together with their low bioavailability hampers the development of therapeutic strategies based DNA or RNA oligonucleotide.

Among the different formulative approaches, the use of nanotechnologies to deliver drugs in cancer therapy is certainly receiving a growing attention. The number of papers published in 2013 on this topic is

of about ten times higher if we compare the number of papers published in one year a decade before (Figure 1).

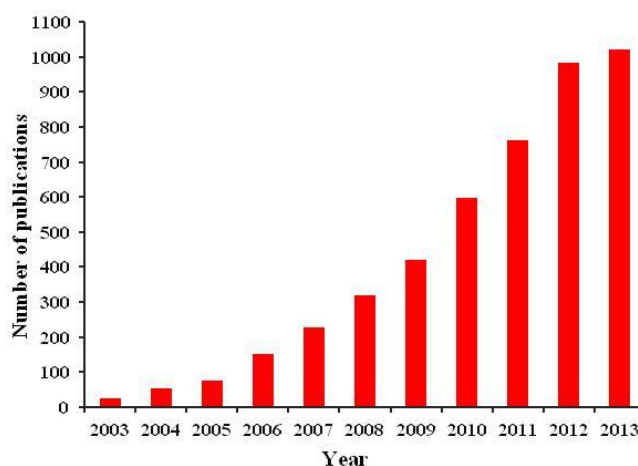


Figure 1. Number of publications in nanotechnology area in the last 10 years (*data from Medline*).

Nanoparticles (NPs) for cancer therapeutics are being introduced in order to overcome several limitations of conventional small-molecule chemotherapeutics and to increase treatment efficacy. Over the past decades, different “first-generation” therapeutic NP-based products are on the market. Liposomes, the first NP platform, have widely demonstrated a significant improvement of the therapeutic benefit of clinically validated drugs by enhancing drug tolerability and/or efficacy. The introduction of liposomes containing anthracyclines in clinic, firstly Daunoxome and then Doxil/Caelyx/Lipodox, significantly changed the landscape of cancer treatment. The encapsulation of doxorubicin in liposome achieved a significant decrease of the cardiotoxicity and enhance the efficacy of doxorubicin even in drug-resistant tumors. Later on, Abraxane and Genexol-PM, respectively albumin NPs and polymeric micelles for the

delivery of Paclitaxel (PXL), were the following classes of therapeutic nanomedicine to be commercialized. Both technologies, when compared to standard PXL (Taxol), demonstrated significantly higher tumor response rates, longer times to tumor progression and avoided the concomitant use of the toxic Cremophore (Gradishar W. J. *et al.*, 2005).

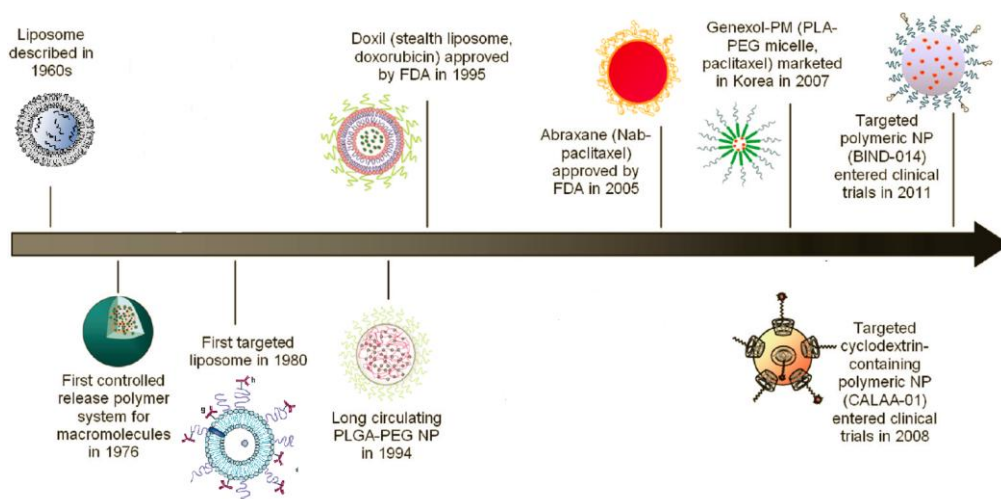


Figure 2. Historical timeline of NPs based products on the market.

In the last decade, the research is moving on the design of “multifunctional” NPs, aimed at increasing the safe and the effectiveness of NPs. Paul Ehrlich, the “father of chemotherapy”, approximately a century ago introduced the concept of a “magic bullet” referring to a drug that can selectively attach diseased cells avoiding health cells (Strebhardt K. *et al.*, 2008). Several strategies can be approached to allow a drug to reach a specific target. Among all, the conjugation of targeting ligands to the surface of the NPs have been proposed in order to increase the selectivity of the NPs towards cancer cells also increasing the intracellular uptake (Gary-Bobo M. *et al.*, 2013; Crommelin D.J. *et al.*, 2013; Lammers T., 2008). In addition, NPs can be modified for targeting specifically not only

cancer cells but also tumors surrounding impermeable biological barriers such as the blood brain barrier (BBB). Chemotherapy for brain tumors has been of limited value because of the low transport ratio of drugs across the BBB. Besides the physiological barrier restriction, the inability of certain drugs to cross the BBB is also caused by MDR proteins over-expressed on this endothelial barrier, with consequent high drug efflux from the brain (Demeule M. *et al.*, 2001). A powerful approach to treat brain disorders could be to combine in one nanosystem tumor targeting strategy, gene therapy and chemotherapy. Lui *et al.*, developed transferrin targeted-dendrimers co-loaded with doxorubicin and TRAIL in the hope of developing an effective treatment for glioma. This combination of treatments demonstrated an increased accumulation of NPs in tumor site together with an enhancement of survival of animals and reduction of unwanted toxicities (Liu S. *et al.*, 2012).

The ability of certain NPs to co-encapsulate multiple therapeutics have been successful in reversing the MDR in cancer. In the recent years, several types of NPs co-loaded with multiple chemotherapeutic agents have been well characterized and have demonstrated improved anti-cancer activity. Yadav S. *et al.*, (2009) demonstrated enhanced PXL cytotoxicity in a resistant SKOV3 cell lines by using polymeric NPs co-loaded with PXL and a siRNA silencing MDR-1. Wu *et al.*, formulated a transferrin conjugated liposomes containing doxorubicin and verapamil (a P-gp inhibitor). They showed enhanced cytotoxicity by overcoming the P-gp-mediated MDR in resistant K562 cells (Wu J. *et al.*, 2007).

Despite the success of these strategies suggested by the introduction of nanotechnology-based products on the market, the wide medical

applications of these systems has been hindered due to the narrow range of active molecules (e.g., broad range of small molecules, proteins, and nucleic acids) clinically validated in “nanotechnological form”. This could be correlated to different reasons, such as doubtful superiority of some formulations, e.g. Doxil, in terms of antitumor efficacy compared to the free drug. Moreover, even when the results obtained from preclinical experiments encourage to move to the clinical phase of the study, the scale-up as well as the preparation of these products in a Good Manufacturing Practice quality is difficult to achieve.

Recently, to address these problems, studies have been focused on the possibility to develop self-assembling nanosystems to overcome stability and scale-up issues (Doll T.A. *et al.*, 2013; Jeong J.H. *et al.*, 2011; Torchilin V.P., 2007; Chaturvedi K. *et al.*, 2011). Interestingly, a product consisting in a self-assembling nanocarrier for siRNA delivery arrived in clinic and concluded the phase I of evaluation (Davis M.E., 2009).

It can be expected that, in the next future, by using the “self-assembling approach” new nanotechnology-based products will get clinical phase of study more easily. On the light of these considerations, in order to have a concrete impact in the treatment of cancer and on the health of patients, a more detailed study of the potentialities of the “self-assembling approach”, i.e. to overcome MDR and/or the BBB, should be a priority.

Objective

The main objective of the research activity was the development of new self-assembling formulations based on nanotechnology for the delivery of active agents in tumors. The first part of the work, was carried out in the laboratories of pharmaceutical technology of the Department of Pharmacy, Università degli Studi di Napoli Federico II, while the second part was done at the Department of Pharmaceutical Sciences, Northeastern University of Boston (USA). The research activity was articulated on two main projects summarized as follows:

1. Design of self-assembling NPs actively functionalized with human transferrin for the delivery of zoledronic acid in brain tumors.
2. Development of multifunctional polymeric micelles for the co-delivery of an anti-survivin siRNA and Paclitaxel for the reversal of drug resistance in ovarian cancer.

In both projects, we proposed and developed particularly promising approaches which combined four crucial elements in one “ultimate NP”:

1. Use of simple and reproducible methods to prepare the formulations in order to develop NPs easily to scale-up;
2. Excellent physical characteristics of the NPs, in terms of incorporation efficiency of the different agents, and size suitable to be systemically used for tumor targeting;
3. Significant inhibition of the cell growth and marked biological effects in different cancer cells by using the developed NPs, superior to that obtained with free drugs;

4. Efficacy of the developed NPs encapsulating the active molecules on the inhibition of the tumor growth of xenograft animal models of different tumors.

Chapter 1

**“Transferrin targeted-self-assembling nanoparticles
containing zoledronic acid: a new strategy for the
treatment of brain tumors”**

Summary

Glioblastoma multiform (GBM) is the most common and aggressive primary malignant brain tumor. Despite the progress in the areas of radiotherapy and chemotherapy, GBM remains a very difficult cancer to treat. Here, to open a new scenario for the treatment of GBM, we have proposed a new strategy for the use of zoledronic acid (ZOL) in brain tumors. ZOL, a third generation bisphosphonate, is a breakthrough for the treatment of bone diseases. In the past decade, several studies have reported a potent anti-cancer activity of ZOL in a wide range of cancer cell lines. Earlier, we have demonstrated, in different animal models of cancer, a mighty anti-tumor activity by encapsulating ZOL in nanoparticles (NPs). Here, in order to improve the target of ZOL to GBM tumor cells and to allow the NPs to overcome the blood brain barrier (BBB), we have designed transferrin (Tf)-targeted self-assembled NPs incorporating ZOL, here named Tf-PLCaPZ NPs. The ability of the developed nanopreparations to bind Tf receptors on cells, to be uptaken by GBM tumour cells was investigated by FACS and confocal microscopy analysis in LN229, U373MG and U87MG, GBM cell lines. Then, in the same cell lines, we have evaluated the effect of the functionalized NPs on the cell growth inhibition by MTT assay. Confocal microscopy and FACS analysis showed that in LN229 cells, GBM expressing the highest degree of Tf-receptor, a significant uptake of Tf-PLCaPZ NPs was achieved. Interestingly, the cell penetration of Tf-PLCaPZ NPs was much higher than the one observed after treatment with no functionalized NPs (PLCaPZ NPs). Moreover, Tf-PLCaPZ NPs induced an oligodendrocytic differentiation in this cell line. The potentiation of anti-proliferative activity

of Tf-PLCaPZ NPs was equal (LN229) or less (U373MG and U87MG) if compared to PLCaPZ NPs and was correlated with Tf receptor expression on tumour cells. In a second step, we have investigated the potential of a combined therapy of temozolomide (TMZ), a gold standard for the treatment of GBM, and Tf-PLCaPZ NPs. The results revealed that, in LN229 cells the sequential therapy of TMZ and Tf-PLCaPZ NPs leading to superior therapeutic activity compared to their single administration.

Finally, we have evaluated the activity of Tf-PLCaPZ NPs in an orthotropic model of nude mice xenografted with U373-MG GBM cells. Interestingly, the treatment with Tf-PLCaPZ NPs elicited the highest anti-cancer activity compared to all the other treatment groups.

Introduction

GBM are highly aggressive brain tumors with poor clinical outcome. Despite a broad range of new and more specific treatment strategies, the therapy of GBM remains challenging and tumors relapse in all the cases. The main limit of conventional chemotherapy in the treatment of brain tumors is the inability of most of the anti-cancer agents, when intravenously administrated, to reach effective concentration within the brain parenchyma. The BBB protects brain from toxicological injuries but, at the same time, makes impossible the crossing of the most of therapeutic agents in the brain. Only highly lipophilic molecules can passively diffuse through BBB to reach central nervous system (CNS).

On the light of these considerations, it has become extremely important to develop suitable dosage form capable to sensitize brain tumors to conventional therapies (Chinot O.L. *et al.*, 2013; Zhu J.J. *et al.*, 2013). Moreover, the potential to use new agents, such as ZOL, should be investigated.

ZOL belongs to the nitrogen containing bisphosphonates (NBPs), agents of choice for the treatment of bone metastases. ZOL inhibits the farnesyl pyrophosphate synthase (FPPS), the upstream enzyme involved in the cholesterol synthesis chain, (Aparicio A. *et al.*, 1998; Senaratne S.G. *et al.*, 2000; Lee M.V. *et al.*, 2001; Schafer W.R. *et al.*, 1992), with consequent inhibition of cell proliferation, differentiation, adhesion and tumorigenesis (Caraglia M. *et al.*, 2006). Due to these pharmacodynamic effects, ZOL has widely demonstrated a direct anti-proliferative action on human tumor cells in vitro (Caraglia M. *et al.*, 2004). Unfortunately, ZOL has a very short

plasma half-life and tends to accumulate in the bone, which results in far below therapeutically effective levels that reach tumor tissues (Chen T. *et al.*, 2002; Skerjanec A. *et al.*, 2003). Therefore, new approaches aimed at increasing ZOL plasma half-life and achieve effective concentrations of ZOL in different districts, such as tumors, must be designed (Caraglia M. *et al.*, 2006). To address this problem, previously we proposed a new nanopreparation for the delivery of ZOL in solid tumors. In particular, NPs made by a mixture of calcium phosphate NPs (CaP NPs) and PEGylated cationic liposomes were developed by using self-assembling processes. The developed formulation exhibit optimal physical characteristics together with the possibility to prepare the NPs immediately before use, overcoming problems of stability during the storage which often hampers the scale-up of many promising drug delivery systems (Salzano G. *et al.*, 2011). In addition, in *in vivo* model of prostate adenocarcinoma, a strong and significant inhibition of the tumor growth was demonstrated (Marra M. *et al.*, 2012).

In this study, in order to investigate the potential of ZOL also in the treatment of aggressive GBM tumors, we upgraded the previous developed NPs by introducing human Tf on the surface. The introduction of specific ligands on the surface of NPs offers the chance of improving the efficacy and specificity of therapeutics in certain diseases as well as to enhance the access of the NPs to impermeable barriers, such as the BBB. (Patel M.M. *et al.*, 2009; Korfel A. *et al.*, 2007).

Here, we described the development and the physical characterization of Tf-PLCaPZ NPs, in terms of size distributions and surface proprieties of the NPs after introduction of Tf. Then, we investigated the ability of the

Tf-PLCaPZ NPs to bind Tf receptors that are over-expressed on GBM cells. Besides, the hemolytic activity of the nanopreparations was evaluated on human blood cells. The effect of Tf-PLCaPZ NPs on the growth inhibition of GBM cells was studied and compared to non-targeted PLCaPZ NPs. In addition, in the same cells, we investigated the mechanisms on the cell death induced by Tf-PLCaPZ NPs and the ability of the developed NPs to potentiate the anti-proliferative activity of TMZ, an anti-cancer agent conventionally used for the treatment of GBM patients. Finally, the anti-tumoral effects of Tf-PLCaPZ NPs, on intracranially human GBM xenografts, have been evaluated.

Materials and methods

Materials

Unless otherwise stated, all chemicals were from Sigma-Aldrich (Saint Louis, MO, USA). 1,2-dioleoyl-3-trimethylammonium-propane chloride (DOTAP) and 1,2-diacyl-sn-glycero-3-phosphoethanolamine-N-[methoxy(polyethylene-glycol)-2000] (DSPE-PEG₂₀₀₀) were obtained from Lipoid GmbH (Cam, Switzerland). 23-(dipyrometheneboron difluoride)-24-norcholesterol (CHOL BODIPY) was purchased from Avanti Polar Lipids. RPMI 1640, DMEM and FBS were purchased from FlowLaboratories (Milan, Italy). Tissue culture plasticware was from Becton Dickinson (Lincoln Park, NJ, USA). Rabbit antisera raised against α -tubulin and CD71 were purchased from Santa Cruz Biotechnology (Santa Cruz, CA, USA). ZOL was kindly provided by Novartis (Novartis, Basilea, Switzerland).

Preparation of self-assembled NPs encapsulating ZOL

Self-assembly NPs encapsulating ZOL, so-called PLCaPZ NPs, were prepared starting from a ZOL aqueous solution, calcium/phosphate nanoparticles (CaP NPs) and PEGylated cationic liposomes.

CaP NPs were prepared as follows. An aqueous solution of calcium chloride (18 mM) was added, dropwise and under magnetic stirring, to an aqueous solution on dibasic hydrogen phosphate (10.8 mM). The pH of both solutions was adjusted beforehand to 9.5 with NaOH. The resulting suspension was filtered through a 0.22 μ m filter (0.22 μ m pore size, polycarbonate filters, MF-Millipore, Microglass Heim, Italy) and then

stored at 4°C before use. To complex ZOL with CaP-NPs (CaPZ-NPs), an aqueous solution containing the amino-bisphosphonate (50 mg/ml) was mixed with the CaP NP dispersion, at a volume ratio of 50:1, respectively.

PEGylated cationic liposomes consisting of DOTAP/chol/DSPE-PEG₂₀₀₀ (1:1:0.5) were prepared by hydration of a thin lipid film followed by extrusion. Briefly, the lipid mixture were dissolved in 1 ml of a mixture chloroform/methanol (2:1 v/v), the resulting solution was added to a 50 ml round-bottom flask, and the solvent was removed under reduced pressure by a rotary evaporator (Laborota 4010 digital, Heidolph, Schwabach, Germany) under nitrogen atmosphere. Then, the lipid film was hydrated with 1 ml of 0.22 µm filtered distilled water and the resulting suspension was gently mixed in the presence of glass beads until the lipid layer was removed from the glass wall, after that the flask was left at room temperature for still 2 h. The liposome suspension was then extruded using a thermobarrel extruder system (Northern Lipids Inc., Vancouver, BC, Canada) passing repeatedly the suspension under nitrogen through polycarbonate membranes with decreasing pore sizes from 400 to 100 nm (Nucleopore Track Membrane 25 mm, Whatman, Brentford, UK). After preparation, liposomes were stored at 4°C. Each formulation was prepared in triplicate.

Equal volumes of suspensions containing DOTAP/chol/DSPE-PEG₂₀₀₀ liposomes and CaPZ NPs, respectively, were mixed in a glass tube and the resulting dispersion was allowed to stand at room temperature for 10 min (PLCaPZ NPs). In particular, 500 µl of CaPZ NPs were added dropwise to 500 µl of DOTAP/chol/DSPE-PEG₂₀₀₀ in a glass tube.

Preparation of self-assembled NPs encapsulating ZOL functionalized with human Transferrin

Tf-modified PLCaPZ NPs were prepared as follows. In a first step, PEGylated cationic liposomes consisting of DOTAP/chol/DSPE-PEG₂₀₀₀ (1:1:0.5 weight ratio) were prepared by hydration of a thin lipid film as reported above. In a second step, pre-formed PEGylated cationic liposomes were mixed with human Tf (10 mg/ml in phosphate buffer at pH 7.4) at a volume ratio of 1:1, at room temperature for 15 min, obtaining the so-called Tf-PEGylated cationic liposomes. Separately, CaP NPs containing ZOL were prepared as reported above. (Salzano G. *et al.*, 2011). Finally, Tf-PLCaPZ NPs were obtained by mixing Tf-PEGylated cationic liposomes complex with CaPZ NPs, at a volume ratio of 1:0.5, at room temperature for 15 min. Plain Tf-modified NPs (Tf-PLCaP NPs), ZOL-encapsulating NPs without Tf (PLCaPZ NPs) and plain PLCaP NPs were prepared similarly. Each formulation was prepared in triplicate. For intracellular penetration studies, fluorescently labeled NPs containing 0.1% (w/w) of CHOL BODIPY were prepared similarly by adding the fluorescent cholesterol in the lipid mixture of DOTAP/chol/DSPE-PEG₂₀₀₀ during the liposomes preparation.

Characterization of PLCaPZ NPs and Tf-PLCaPZ NPs

The mean diameter of NPs was determined at 20°C by photon correlation spectroscopy (PCS) (N5, Beckman Coulter, Miami, USA). Each sample was diluted in deionizer/filtered water (0.22 µm pore size, polycarbonate filters, MF-Millipore, Microglass Heim, Italy) and analyzed with detector at 90° angle. As measure of the particle size distribution, polydispersity

index (P.I.) was used. For each batch, mean diameter and size distribution were the mean of three measures. For each formulation, the mean diameter and P.I. were calculated as the mean of three different batches. The zeta-potential (ζ) of the NPs surface was measured in water by means of a Zetasizer Nano Z (Malvern, UK). Data of ζ were collected as the average of 20 measurements. ZOL analysis was carried out by reverse phase high performance liquid chromatography (RP-HPLC) as previously reported (Salzano G. *et al.*, 2011). The incorporation efficiency of ZOL in Tf-PLCaPZ NPs was determined as follows: 1 ml of NPs dispersion was ultracentrifugated (Optima Max E, Beckman Coulter, USA) at 80.000 rpm at 4°C for 40 min. Supernatant was carefully removed and analyzed to determine un-incorporated ZOL concentration by RP-HPLC. The results have been expressed as complexation efficiency, calculated as the ratio between the amount of ZOL present in the supernatant and the amount of ZOL theoretical loaded.

Hemolysis assay

Hemolysis assay was performed on fresh human blood as previously reported by Cheng C. *et al.* (2008) with slight modifications. The erythrocytes were collected by centrifugation at 2000 rpm for 15 min, and then washed three times with phosphate buffered saline (PBS) buffer at pH 7.4. The stock dispersion was prepared by mixing 3 mL of centrifuged erythrocytes into 11 mL of PBS. Then, 100 μ l of stock dispersion were added to 1 mL of NPs dispersions, prepared as reported above and incubated for 4 h at 37°C under slightly agitation. The percentage of hemolysis was determined by UV–vis analysis of the supernatant at 541 nm absorbance after centrifugation at 13,000 rpm for 15 min. Plain Tf-PLCaP

NP, PLCaPZ NP without Tf, plain Tf-PLCaP NP and ZOL free at a final concentration of 20 µg were used as controls. One milliliter of PBS was used as the negative control with 0% hemolysis, and 1 mL of deionized water was used as the positive control with 100% hemolysis. All hemolysis data were calculated using the following formula:

$$\text{Hemolysis \%} = (\text{Abs}-\text{Abs0})/(\text{Abs100}-\text{Abs0})*100$$

Cell lines, protein extraction and western blotting

Tf receptor (CD71) was evaluated in three different cell lines of human GBM, LN229, U87 MG and U373 MG by Western Blotting method. GBM cell lines were provided by Dr. C. Leonetti (Department of Experimental Oncology, Regina Elena National Cancer Institute IRCCS - Rome) and were grown in medium as suggested by ATCC in a humidified incubator containing 5% CO₂ at 37°C. Cell cultures were washed twice with ice-cold PBS/BSA, scraped, and centrifuged for 30 min at 4°C in 1 ml of lysis buffer (1% Triton, 0.5% sodium deoxycholate, 0.1M NaCl, 1mM EDTA, pH 7.5, 10mM Na₂HPO₄, pH 7.4, 10mM PMSF, 25mM benzamidin, 1mM leupeptin, 0.025 U/ml aprotinin). Equal amounts of cell proteins, assessed by Lowry assay using bovine serum albumin as standard, were separated by SDS–PAGE. The proteins on the gels were electrotransferred to nitrocellulose and reacted with the different antibodies as previously shown (Marra M. *et al.*, 2009).

Analysis of NPs intracellular distribution by FACS and confocal microscopy

A BD FACS Calibur fluorescent-activated flow cytometer and the BD CellQuest software (BD Biosciences) were used to perform flow cytometry analysis. Fluorescent-labeled NPs were incubated with LN229 cells in medium with at final concentration corresponding to their IC50 at 72 h. After 1, 3, 6, 24, 48 and 72 h of incubation at 37 °C, removal of attached NPs was accomplished by washing the cells with PBS at pH 7.4 for 1 min. Cells were then detached by trypsinization. The samples were subsequently washed twice and for each sample, 10,000 cells were measured with a FACScalibur flow cytometer (Becton Dickinson) using the CellQuest software (Becton Dickinson). After 6h and 72h of incubation of LN229 cells with fluorescently labeled NPs, the cells were fixed for 20 minutes with a 3% (w/v) paraformaldehyde (PFA) solution and permeabilized for 10 minutes with 0.1% (w/v) Triton X-100 in phosphate-buffered saline (PBS) at room temperature. To prevent nonspecific interactions of antibodies, the cells were treated for 2 hr in 5% bovine albumin serum (BSA) in PBS, then the cells were incubated with a specific mouse monoclonal Ab raised against vimentin (1:1,000 in blocking solution, 3% (w/w) BSA in TBS-Tween 0.1%, Sigma) for 2 hours at 37 ° C. After several washes the cells were incubated with a secondary IgG goat anti-mouse antibody (Alexa Fluor 633, Life Technologies, Carlsbad, CA) diluted 1:1,000 in blocking solution for 1 h at room temperature. The slides were mounted on microscope slides by Mowiol. The analyses were performed with a Zeiss LSM 510 microscope equipped with a plan-apochromat objective X 63 (NA 1.4) in oil immersion. The fluorescences

of the Alexa 488 and Alexa 633 were collected in multi-track mode using BP505-530 and LP650 as emission filters, respectively.

Confocal Microscopy Analysis of Double Immunofluorescence

LN229 cells were treated with free ZOL or the different NPs formulations at a concentration equal to their IC50 at 72h. The cells were fixed for 20 minutes with a 3% PFA solution and permeabilized for 10 minutes with 0.1% (v/v) Triton X-100 in PBS at room temperature. To prevent nonspecific interactions of antibodies, the cells were treated for 2 hr in 5% (w/v) BSA in PBS, then the cells were incubated with a specific mouse monoclonal Ab raised against Vimentin (1:1000 in blocking solution, 3% BSA in TBS-Tween 0.1%, mouse, Sigma) for 2 hours at 37 ° C. After several washes the cells were incubated with a secondary IgG goat anti-mouse antibody (Alexa Fluor 633, Life Technologies, Carlsbad, CA) diluted 1:1,000 in blocking solution for 1 h at room temperature. Subsequently, the cells were washed with PBS and incubated with specific rabbit polyclonal Ab against either glial fibrillary acidic protein (GFAP) (Ab7260, Abcam, Cambridge, United Kingdom) or the oligodendrocyte lineage genes 2 (Olig2) (Ab77953, Abcam, Cambridge, United Kingdom) diluted 1:1,000 in blocking solution, at 4 °C o/n. After additional washes, the cells were incubated with both a secondary IgG goat anti-mouse antibody (Alexa Fluor 633, Life Technologies, Carlsbad, CA) and a goat polyclonal anti-rabbit antibody (Alexa 488, Life Technologies, Carlsbad, CA) diluted 1:1,000 in blocking solution for 1 hour at room temperature. The slides were mounted on microscope slides by DAPI. The analysis was performed with a Zeiss LSM 510 microscope equipped with a plan-apochromat objective X 63 (NA 1.4) in oil immersion. The fluorescences

of the Alexa 488 and Alexa 633 were collected in multi-track mode using BP505-530 and LP650 as emission filters, respectively.

Cell proliferation by MTT assay

After trypsinization, all cell lines were plated in 100 μ L of medium in 96-well plates at a density of 2×10^3 cells/well. One day later the cells were treated with free ZOL, Tf-PLCaPZ NPs, plain Tf-PLCaP NPs, PLCaPZ NPs and plain PLCaP NPs at concentrations ranging of ZOL from 0,78 to 120 μ M. Cell proliferation was evaluated by MTT assay as previously described (Marra M. *et al.*, 2009).

Drug combination studies

For the evaluation of the synergism between the different NP formulations or free ZOL and TMZ on the growth inhibition of GBM cells, the cells were seeded in 96-multiwell plates at the density of 2×10^3 cells/well. After 24 h of incubation at 37°C the cells were treated with different concentrations of Tf-PLCaPZ NPs, PLCaPZ NPs, free ZOL, TMZ. Alternatively, cells were treated simultaneously with TMZ and NP formulations or sequentially with TMZ followed by NP formulations and conversely. The evaluation of synergism was performed using dedicated software, CalcuSyn (Biosoft, Ferguson, MO), which measures the interaction between the drugs by calculating the indexes of combination (CIs). CI values <1, 1 and> 1 indicate synergism, additivity and antagonism, respectively. Drug combination studies were based on concentration-effect curves generated as a plot of the fraction of unaffected (surviving) cells vs. drug concentration after 72 h of treatment. Assessment of synergy was performed analyzing drug interaction by the CalcuSyn

computer program (Biosoft, Ferguson, MO). Furthermore, we analyzed the specific contribution of the different NPs, free ZOL and TMZ on the cytotoxic effect of the combinations by calculating the potentiation factor (PF), defined as the ratio of the IC50 of either NPs, free ZOL and TMZ alone to the IC50 of the different combinations; a higher PF indicates a greater cytotoxicity.

In vivo: Therapeutic efficacy in a heterotopic and orthotopic model of GBM

Cell line

Human U373MG GBM cells were transfected with pcDNA3-luc (U373MG-LUC) as previously described (Nardinocchi L. *et al.*, 2010) and were grown in RPMI medium in a humidified incubator containing 5% CO₂ at 37°C.

In vivo experiments

CD-1 male nude (nu/nu) mice, 6–8 weeks old and weighing 22–24 g were purchased from Charles River Laboratories (Calco, Italy). The procedures involving mice and care were in compliance with Regina Elena National Cancer Institute animal care guidelines and with international directives (directive 2010/63/EU of the European parliament and of the council; Guide for the Care and Use of Laboratory Animals, United States National Research Council, 2011). For heterotopic experiments, immunosuppressed mice were injected intramuscularly (i.m.) into the hind leg muscles of mice at 3×10^6 U373MG-LUC GBM cells /mouse. After 6 days (when a tumor mass of about 300mg was evident) mice were randomized, divided in five

groups and treatment started. The following groups were evaluated: untreated; free ZOL; plain Tf-PLCaP NPs; ZOL-containing Tf-PLCaPZ NPs, and ZOL-containing PLCaPZ NPs without Tf. Mice were treated intravenously (i.v.) with the different NP formulations or with 20 µg of free ZOL, for three times a week for 3 consecutive weeks. This scheduling of treatment was chosen based on previous published experiments (Marra M. *et al.*, 2012). Tumor sizes were measured three times a week in two dimensions by a caliper and tumor weight was calculated using the following formula: $a \times b^2 / 2$, where a and b are the long and short diameter of the tumor, respectively. Antitumor efficacy of treatments was assessed by the following end-points: a) percent tumor weight inhibition (TWI%); b) tumor growth delay, evaluated as T - C, where T and C are the median times for treated and control tumors, respectively, to achieve equivalent size; c) complete tumor regression, defined as tumor disappearance, as evaluated by palpability, lasting for at least 10 days during or after treatment period; d) increase of mice survival by euthanizing the animals, for ethical reasons, when the tumors reached 3 g in weight; e) stable disease, defined as the maintenance for at least three weeks of the same tumor weight as the start of treatment; f) complete response, defined as the disappearance of tumor, for at least three weeks in the course of treatment. Each experimental group included six mice and experiments were repeated at least twice.

For orthotopic experiments, mice were anesthetized with a combination of tiletamine–zolazepam (Telazol, Virbac, Carros, France) and xylazine (xylazine/ Rompun BAYER) given intramuscularly at 2 mg/kg and injected intracranially with U373 MG-LUC cells at 2.5×10^5 cells/mouse, through

the center-middle area of the frontal bone to a 2-mm depth, using a 0.1 mL glass microsyringe and a 27-gauge disposable needle. One hour prior to intracranial implantation, the mice were weighed and pre-medicated with an orally administration of 0.5 mg/ kg/d of Metacam (meloxicam) in saline to control for post-operative pain and inflammation. The medication was carried out until the end of the experiment. Animals were closely monitored by visual inspection and weighed daily from start of treatment and sacrificed when signs of tumor burden (especially weight loss >20% and severe neurological dysfunction) were evident. The time to this moment since GBM cells injection is considered as 'survival time'. Mice were treated i.v., starting at day 8 after cells injection, with plain Tf-PLCaP NPs, Tf-PLCaPZ NPs and PLCaPZ NPs at 20 µg/mouse of ZOL for three time a week for 3 consecutive weeks. Experiments with ZOL free were not performed due to the well-known inability of this drug to cross the BBB. Each experimental group included eight mice and experiments were repeated twice.

Bioluminescence imaging analysis

Mice bearing intra brain U373MG-LUC tumors were imaged using the IVIS imaging system 200 series (Caliper Life Sciences, Hopkinton, MA, USA). Briefly, mice were anesthetized with a combination of tiletamine–zolazepam (Telazol, Virbac, Carros, France) and xylazine (xylazine/Rompun BAYER) given intramuscularly at 2 mg/kg. Then mice were injected intraperitoneally with 150 mg/kg D-luciferin (Caliper Life Sciences), and imaged in the supine position 10 min after luciferin injection. Imaging was performed at baseline before the start compound administration and several times during the experiment. Data were

acquired and analyzed using the living image software version 3.0 (Caliper Life Sciences).

Statistical analysis

For comparison of several groups, one-way ANOVA for multiple groups, followed by Newman-Keuls test if $P < 0.05$ was performed using the GraphPad Prism version 5.0 software (GraphPad Software, Inc, San Diego,CA). All numerical data are expressed as mean \pm SD, $n = 3$ or more, from 3 different experiments. Any p values less than 0.05 was considered statistically significant.

Results

Here, in order to improve the specificity and the delivery of ZOL in GBM cells, we upgraded the earlier developed PLCaPZ NPs with human Tf. The protocol to prepare the PLCaPZ NPs was modified in order to introduce Tf on the NP surface without a significant alteration of the size as well as of the self-assembling characteristics. After a preliminary formulative phase (data not shown), we selected the optimized preparation condition to prepare Tf-PLCaPZ NPs. Physical characteristics of Tf-PLCaPZ NPs, i.e. size, surface charge and ZOL loading efficiency, are shown in Table I. When Tf was added to PEGylated cationic liposomes, a dramatic decrease in the net positive charge of the liposomes was observed. No significant change in the particles mean diameter as well as in the size distribution of the NPs was observed after functionalization of the PLCaPZ NPs with Tf. In particular, Tf-PLCaPZ NPs had a mean diameter of about 147 nm with a very narrow size distribution ($PI < 0.2$). Furthermore, chromatographic analysis of non-complexed ZOL showed an actual loading of $\sim 100 \mu\text{g}$ of ZOL/mg lipids, corresponding to a complexation efficiency of about 100%, in both PLCaPZ NPs and Tf-PLCaPZ NPs (data not showed).

Formulations	Diameter (nm) \pm SD	I.P. \pm SD	$\zeta \pm$ SD
PLCaPZ NPs	147.5 \pm 7.1	0.152 \pm 0.06	+17.5 \pm 5.6
PEGylated cationic liposomes	140.0 \pm 15.0	0.149 \pm 0.04	+47.37 \pm 3.5
Tf-PEGylated cationic liposomes complex	142.4 \pm 21.1	0.152 \pm 0.08	+7.5 \pm 2.0
Tf-PLCaPZ NPs	147.7 \pm 15.0	0.169 \pm 0.05	+11.3 \pm 1.1

Table I. Physical characteristics of the different NP formulations.

Then, in order to evaluate the hemolytic activity of those NPs in human blood, hemolysis assay was performed. Figure 1 shows the hemolytic activity of the developed NPs when added in presence of erythrocytes. Interestingly, in all the cases no significant hemolytic activity was observed after incubation of a dispersion containing erythrocytes with the NPs developed. It is worth to note that after incubation with the NPs functionalized with Tf an additional significant reduction of the hemolytic activity compared to not targeted PLCaPZ NPs ($p < 0.001$) was observed.

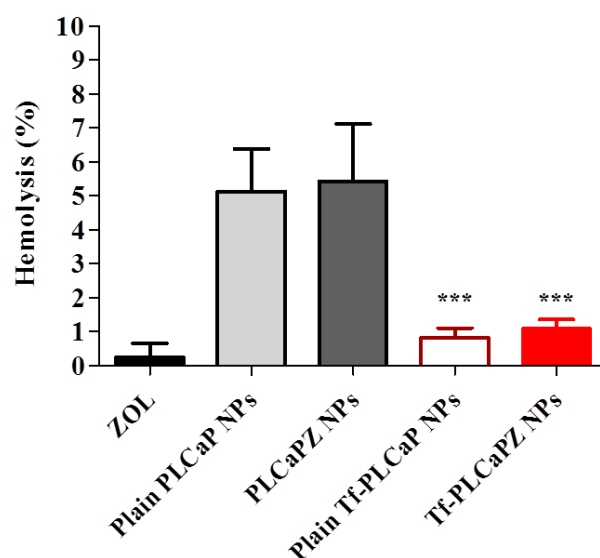


Figure 1. Hemolytic activities of Tf-PLCaPZ NPs. Data represented the means and standard deviations of three independent experiments. P values ($*** < 0.001$) were obtained comparing Tf-PLCaPZ NPs to PLCaPZ NPs.

Expression of Tf receptor in GBM cells and cytotoxicity studies

We have evaluated the anti-proliferative effects of free ZOL and of the different NP formulations on the three GBM cell lines with MTT viability assay. The cells were treated for 72 h and then the viability was evaluated. We have identified the concentration of the drugs able to inhibit the 50% of

cell growth (IC₅₀) (Table II). We observed that the encapsulation of ZOL into NPs increased the cytotoxic activity of ZOL by reducing the IC₅₀. Free ZOL induced a 50% growth inhibition at a concentration of 22, 69.8 and 46 μM (IC₅₀) in LN229, U87 MG and U373 MG, respectively, and this effect was enhanced when ZOL was encapsulated into NPs. In fact, PLCaPZ NPs showed an IC₅₀ equal to 9 μM in LN229, 18 μM in U87 MG and 20 μM in U-373 MG, that was significantly lower than that one induced by free drug (Table II). Tf-PLCaPZ NPs caused a significant decrease of the IC₅₀ compared to free ZOL but not respect to PLCaPZ NPs (11 μM for LN229, 37 μM for U87 MG and 39 μM for U373 MG) (Table II). In all the cases, plain NPs did not induce a significant growth inhibition demonstrating a very low cytotoxicity.

CELL LINES	ZOL (IC ₅₀ μM)	PLCaPZ NPs (IC ₅₀ μM)	Plain PLCaP NPs (IC ₅₀ μM)	Tf-PLCaPZ NPs (IC ₅₀ μM)	Plain Tf-PLCaPZ NPs (IC ₅₀ μM)
LN-229	22 \pm 0.01	9.0 \pm 0.06	>>120 \pm 0.01	11.0 \pm 0.03	>>120 \pm 0.03
U-87 MG	69.8 \pm 0.02	18.0 \pm 0.01	>>120 \pm 0.04	39.0 \pm 0.04	>>120 \pm 0.01
U-373 MG	46.0 \pm 0.04	20.0 \pm 0.03	>>120 \pm 0.03	37.0 \pm 0.02	>>120 \pm 0.07

Table II. IC₅₀ values of NP formulation

Thereafter, we investigated the expression of Tf type 1 receptor (CD71) in GBM cells by Western Blot. LN229, U87 MG and U373 MG cells were harvested after 72h of treatment with ZOL at a concentration equal to its IC₅₀ at 72 h for each cell line. We used prostate cancer cells PC-3 as a positive control. The receptor was expressed in all GBM cell lines at baseline and treatment with ZOL did not significantly modulate TfR expression. As expected, PC-3 expressed the receptor at high levels. The expression of γ -tubulin was assessed as loading control (Figure 2).

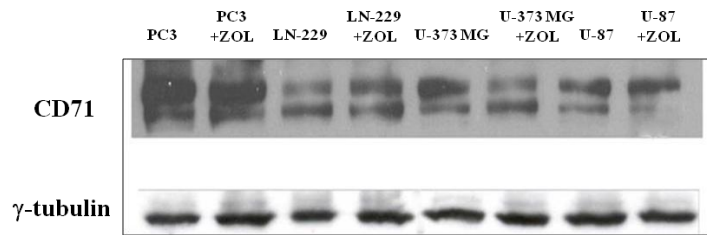


Figure 2. Western Blot analysis of the TfR levels in GBM cells.

On the bases of these results, we evaluated the basal expression of the TfR both on the cell membrane and at the intracellular level on all GBM cell lines by FACS analysis. The receptor was expressed at higher levels in LN229 both on the membrane and at the intracellular level while the U373 MG and U87 MG cells expressed the receptor at lower levels both on the membrane and at intracellular level (Figure 3). Interestingly, LN229 cell line was also the most responsive to the inhibitory effects of Tf-PLCaPZ NPs.

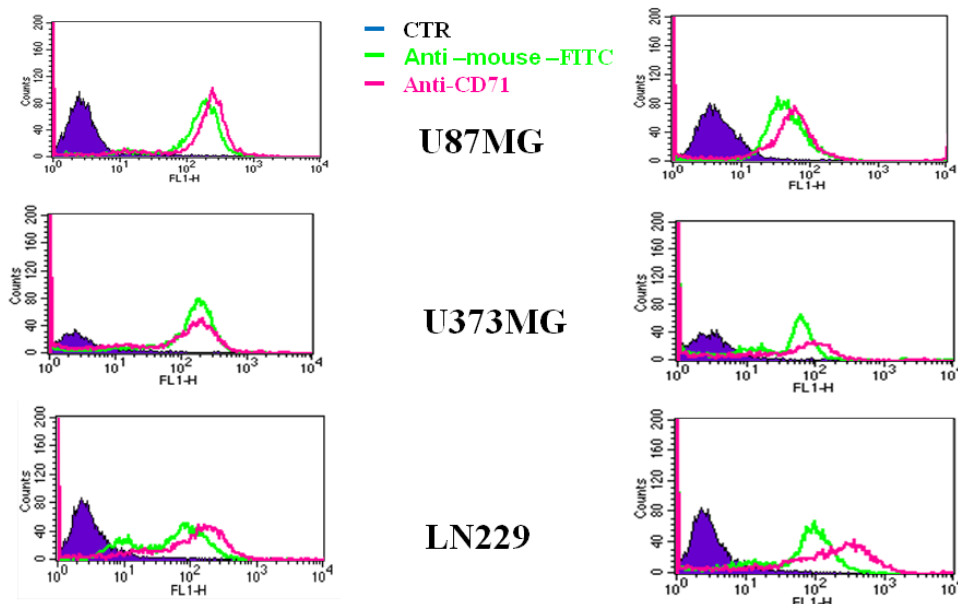


Figure 3. Basal expression of the TfR both on the cell membrane and at the intracellular level on all GBM cell lines by FACS analysis.

Tf-PLCaPZ NPs uptake and intracellular distribution

To investigate the NPs uptake and the intracellular distribution, fluorescently labeled NPs were used on LN229 cells. The fluorescence associated to the cells was evaluated by both FACS and confocal laser scanning microscopy (CLSM). FACS analysis of LN229 cells after 1, 3, 6, 24, 48, and 72h hours of incubation with fluorescently labeled NPs (Figure 4) was performed. In particular, after 6h of incubation with PLCaPZ NPs or Tf-PLCaPZ NPs, FACS analysis revealed the highest increase in the % of mean fluorescence intensity (MFI) associated to the cells, thus showing NPs uptake as compared with the untreated control (Figure 4 A). MFI of control was considered as 100%; after 6h of cell incubation Tf-PLCaPZ NPs induced a significantly higher MFI increase (450%) as compared with PLCaPZ NPs (370%) (Figure 4 B). In both cases, MFIs decreased in a time-dependent manner after 24h.

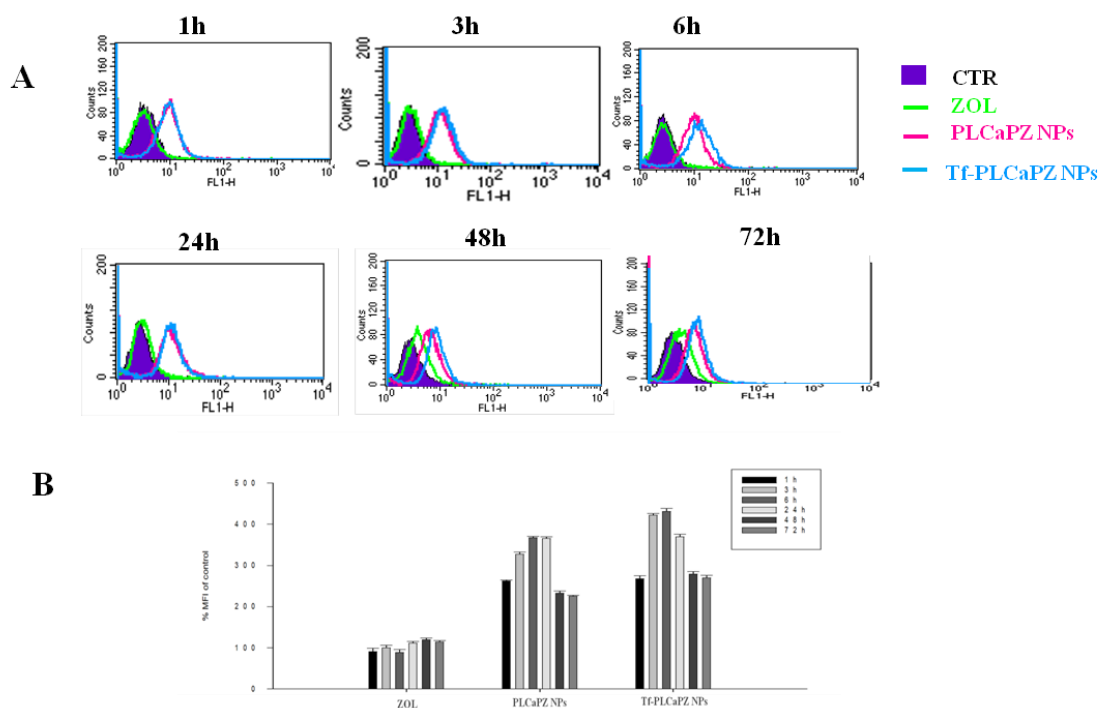


Figure 4. A. FACS analysis of LN229 cells after 1, 3, 6, 24, 48 and 72 h of incubation at 37 °C with Bodipy-labeled NPs. The experiments were performed at least three different times and the results were always similar. **B.** Mean fluorescence intensity (MFI), expressed as % of unexposed cells, of cells exposed to the different NPs formulations.

The uptake and intracellular distribution of fluorescently labeled NPs after 6 and 72h of incubation was studied also by confocal microscopy. After 6h, CLSM results showed a widespread and intense fluorescence, with perinuclear green spots into the cytoplasm, for cells incubated with Tf-PLCaPZ NPs (Figure 5). Cells treated with PLCaPZ NPs, compared to Tf-PLCaPZ NPs, evidenced a significant lower fluorescence intensity. A green fluorescence was observed also in the cells incubated with plain NPs and in particular, plain Tf-PLCaP NPs showed the higher fluorescence intensity (Figure 5). After 72h, the fluorescence intensity decreased in all the cases (Figure 5). Therefore, the intracellular uptake of NPs could contribute to increasing the amount of ZOL that reaches its cytoplasmic targets.

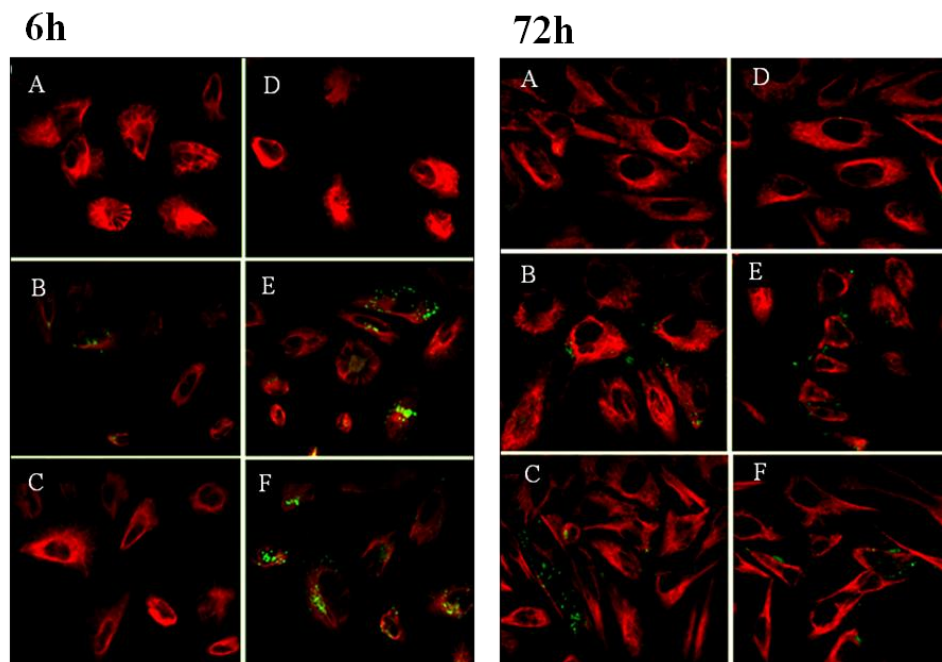


Figure 5. Confocal microscopy images of LN229 after 6 and 72 h of incubation at 37 °C with fluorescently-labeled NPs. Representative images of CTR (A), Plain PLCaP NPs (B), PLCaPZ NPs (C), ZOL (D), Plain Tf-PLCaP NPs (E), Tf-PLCaPZ NPs (F). The cells were visualized with a confocal microscope at magnification 100x.

Effects of Tf-PLCaPZ NPs on the differentiation of GBM cells

After 48h of treatment with Tf-PLCaPZ NPs at a concentration corresponding to its IC50, we observed that LN229 cells changed their shape. In details, Tf-PLCaPZ NPs induced a significant cell elongation that was higher than that one induced by free ZOL and PLCaPZ NPs. As cell elongation can be correlated with cell differentiation, we have studied two differentiation markers, Olig2 and GFAP that were assessed at CLSM. In details, Olig2 showed a well distributed higher fluorescence for cells incubated with Tf-PLCaPZ NPs as compared to free ZOL or PLCaPZ NPs (Figure 6). Cells treated with Tf-PLCaPZ NPs evidenced widespread lower fluorescence intensity for GFAP as compared to Olig2 expression (Figure 6). These data suggest that the treatment of LN229 cells with ZOL induced

a differentiation towards an oligodendrocyte phenotype and that this effect was strongly enhanced by the delivery of the agent by Tf-PLCaPZ NPs.

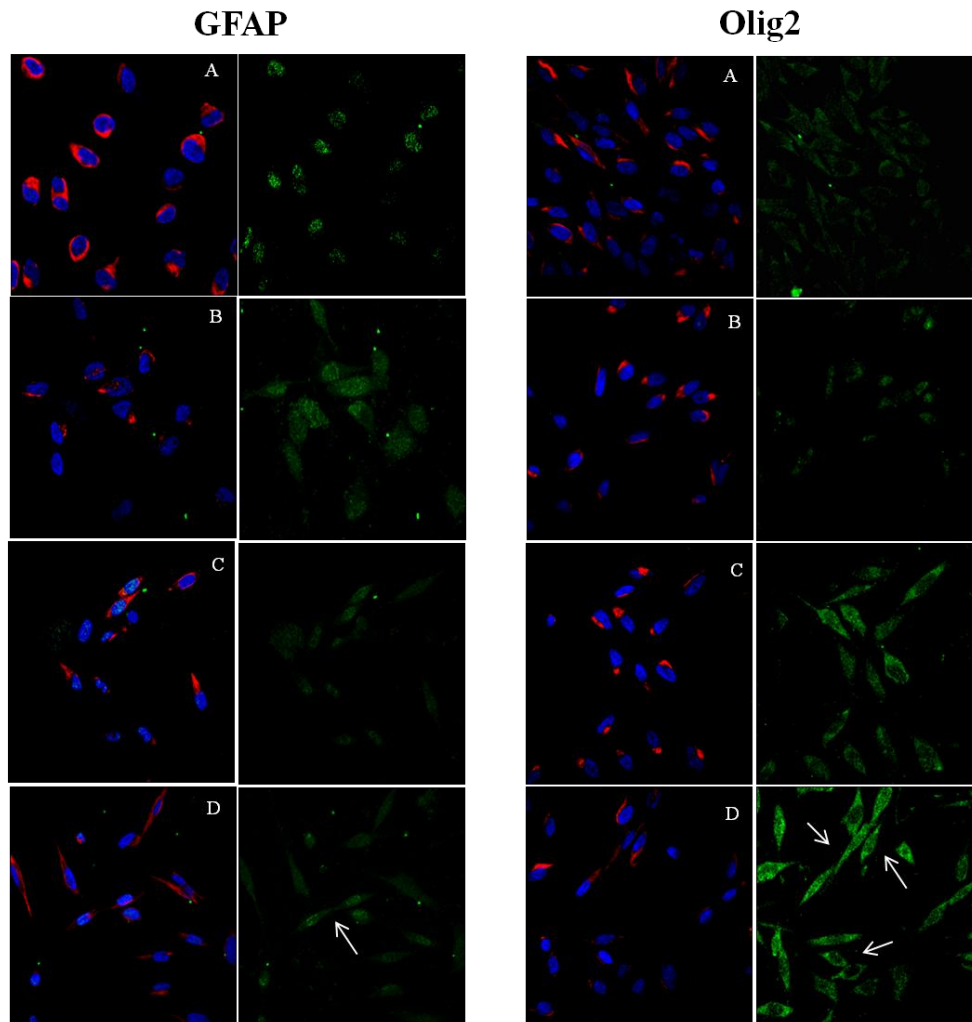


Figure 6. Effects of the NPs on the differentiation of LN229 cells. Confocal microscopy images of LN229 after 48 h of incubation at 37 °C with PBS (A), ZOL (B), PLCaPZ NPs (C) or Tf-PLCaPZ NPs (D) at a concentration equal to their IC50s. The cells were incubated with anti-vimentin antibody (red) (Santa Cruz Biotechnology, Inc.) and either anti-Olig2 antibody (green, right panels) (Abcam) or anti-GFAP antibody (green, left panels) (Abcam) for 1 hour. The slides were mounted with DAPI. The cells were visualized with a fluorescent microscope at magnification (100x). Arrows show examples of fluorescence due to Olig2 or GFAP specific staining.

Anti-proliferative effects of the sequential administration of Tf-PLCaPZ NPs and TMZ on GBM cells

A conventionally used cytostatic agent for the treatment of GBM in combination with radiation therapy or alone after surgery and radiotherapy is TMZ. On these bases, we evaluated the growth inhibition induced by TMZ on the three GBM cell lines. After 72h the IC₅₀s of TMZ were 176 μ M, 95 μ M and 110 μ M for LN-229, U87 MG, U373 MG, respectively (Table III).

CELL LINES	TMZ μ M IC ₅₀
LN-229	176 \pm 0.02
U-87 MG	95 \pm 0.03
U-373 MG	110 \pm 0.02

Table III. IC₅₀ values of TMZ

These data were used to assess the effects of TMZ in combination with the different NP formulations and in different sequences of cell exposure. In details, we added to the cells TMZ for 72 h and NPs for 48h or vice versa or we simultaneously treated the cells with TMZ and NP formulations for 72h. Analyzing the results, when free ZOL or the different NPs were simultaneously added to the cells with TMZ, a significant reduction of the anti-proliferative activity, compared to the administration of the single agents, was observed. A slight synergistic effect was observed only in U-373 MG cells, after treatment with the combinations PLCaPZ NPs/TMZ and Tf-PLCaPZ NPs/TMZ. On the contrary, better results were obtained when TMZ was added to the cells before both free ZOL, PLCaPZ NPs or Tf-PLCaPZ NPs. In this case, a synergistic effect was observed in all the three GBM cell lines (Figure 7C). Interestingly, TMZ followed by Tf-

PLCaPZ NPs was strongly synergistic on LN229 cells ($IC_{50}= 0.42$) (Figure 7C). Similarly, TMZ followed by free ZOL was highly synergistic on the U87 MG cells ($IC_{50} = 0.43$). The reverse sequences (ZOL, PLCaPZ NPs or Tf-PLCaPZ NPs followed by TMZ) were in almost all the cases antagonistic or additive on the inhibition of the proliferation of all the GBM cell lines (Figure 7B). Only the sequences Tf-PLCaPZ NPs/TMZ and PLCaPZ NPs/TMZ were strongly synergistic on the growth inhibition of LN229 and U373 MG cells, respectively, with an $IC_{50} =0.30$ and $IC_{50} = 0.43$, respectively (Figure 7B).

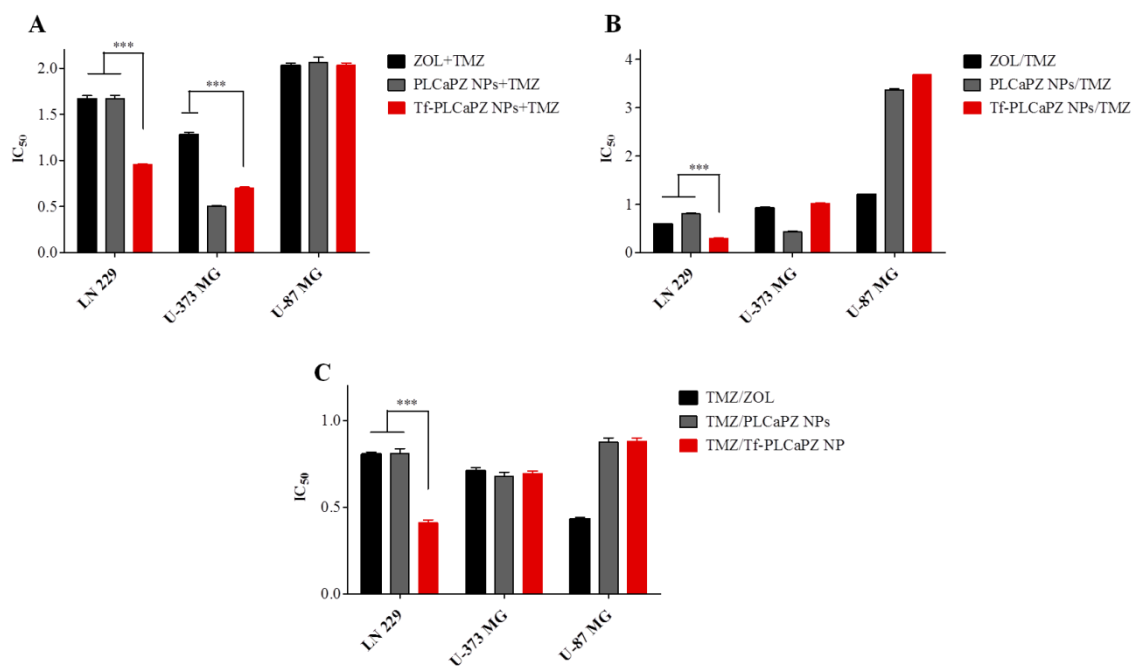


Figure 7. Effects of the TMZ/NPs sequence on the cell growth. **A.** Simultaneous treatment of GBM cell with TMZ and NP formulations. **B.** Sequential treatment of ZOL or NPs formulations followed by TMZ. **C.** Sequential treatment of TMZ followed by ZOL or NPs formulations.

Subsequently, we calculated the potentiation factor (PF) for treatments that showed synergism. The PF is the ratio between the IC_{50} of the drug used alone and the IC_{50} of the drug used in the combination: if PF is greater

than 1, it means that the drug in combination determines its anti-proliferative effect at a lower concentration compared to the drug alone. In our experimental conditions, PF was much more higher when TMZ was added to the cells before the other drugs (ZOL, PLCaPZ NPs, Tf-PLCaPZ NPs) (Table IV). These data suggest that Tf-PLCaPZ NPs strongly potentiated the anticancer effects of TMZ when they are added to the cells after the cytotoxic drug.

Cell lines	TMZ → ZOL	TMZ → PLCaPZ NPs	TMZ → Tf-PLCaPZ NPs
LN - 229	PF _{TMZ} = 3.7	PF _{TMZ} = 4.3	PF _{TMZ} = 12.6
	PF _{ZOL} = 4.0	PF _{PLCaPZ NPs} = 1.4	PF _{Tf-PLCaPZ NPs} = 10.0
U - 373 MG	PF _{TMZ} = 7.3	PF _{TMZ} = 1.5	PF _{TMZ} = 1.4
	PF _{ZOL} = 1.8	PF _{PLCaPZ NPs} = 1.8	PF _{Tf-PLCaPZ NPs} = 10.0
U - 87 MG	PF _{TMZ} = 1.3	PF _{TMZ} = 2.0	PF _{TMZ} = 3.0
	PF _{ZOL} = 1.9	PF _{PLCaPZ NPs} = 3.2	PF _{Tf-PLCaPZ NPs} = 2.2

Table IV. PFs of the synergistic pharmacological combinations.

Antitumor efficacy of Tf-PLCaPZ NPs in heterotopic model of GBM

In order to evaluate the *in vivo* effects of NPs formulations, we inoculated i.m. 3×10^6 U373MG-LUC cells into immunosuppressed mice. U-373MG-LUC cells allow the *in vivo* monitoring of tumor growth by imaging performed as a function of the bioluminescent signal generated by the catalysis of D-luciferin, injected in the animal at the time of imaging. After 6 days, when the tumor mass became palpable and visible by luminescence analysis, the mice were divided into five groups: untreated mice, mice treated with free ZOL, with plain NPs functionalized with Tf, with Tf-PLCaPZ NPs and with plain and PLCaPZ NPs.

In figure 8 are reported the bioluminescence analysis of U373MG-LUC tumors treated with the different formulations. It is evident that Tf-PLCaPZ NPs exhibited the highest antitumor efficacy. In fact, this treatment produced, at nadir of the effect, a significant ($P= 0.009$ vs untreated) tumor weight inhibition of 41%, while the non-functionalized PLCaPZ NPs reduced of 31% the growth of tumors ($P= 0.02$) and free ZOL resulted in a not particularly marked tumor growth inhibition (TWI 20%). The good therapeutic efficacy of Tf-PLCaPZ NPs is also demonstrated by the significant ($P= 0.03$) delay of tumor growth (10 days) and by the increase of life survival of mice (23%). Interestingly, this treatment produced a complete tumor response in 1 out of six mice treated, while PLCaPZ NPs produce a stabilization of disease in 1 out of six mice treated. Finally, it is interesting to note that, all treatments were well tolerated by the animals, as there were no toxic deaths or weight loss in animals (data not showed).

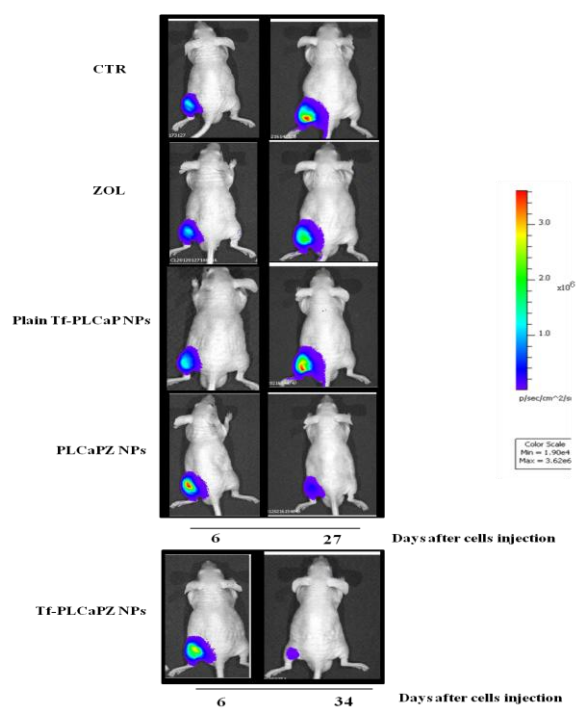


Figure 8. Bioluminescence analysis of a heterotopic model of GBM.

Antitumor efficacy of Tf-PLCaPZ NPs in an orthotopic model of GBM

Based on the promising results obtained *in vitro* and *in vivo*, we subsequently evaluated the therapeutic efficacy of these formulations on orthotopic mice bearing GBM tumors. We inoculated intrabrain 2.5×10^5 U-373MG-LUC cells into immuno-compromised mice. This tumor model closely recapitulated histological phenotypes consistent with those of human GBM. After 8 days, when the tumor mass became visible by bioluminescence analysis, the mice were divided into four groups: untreated mice, mice treated with plain NPs functionalized with Tf, mice treated with Tf-PLCaPZ NPs and mice treated with PLCaPZ NPs. As reported in Figure 9, NPs containing ZOL formulations were effective in limiting the growth of GBM and in particular, Tf-PLCaPZ NPs reduced the tumor mass and elicited the healing of some treated animals. In fact, while all untreated or mice treated with plain NPs showed a progression of the disease, the treatment with NPs containing ZOL produced the stabilization of the disease in 2 out of eight mice treated. Interestingly, Tf-PLCaPZ NPs elicited a more strong antitumor effect determining the stabilization of the tumor mass in 2 out of eight mice and a decrease followed by a complete disappearance of the tumor in 1 out of eight mice. (Figure 9). At this time, six months or more after the end of treatment, mice with complete tumor regression are still alive and in good conditions and bioluminescence analysis did not show the presence of tumor cells in the brain of mice. The higher efficacy of Tf-PLCaPZ NPs than PLCaPZ NPs was demonstrated by the increase of overall survival of mice (23 vs 13%, respectively), while plain Tf-PLCaP NPs treatment was ineffective.

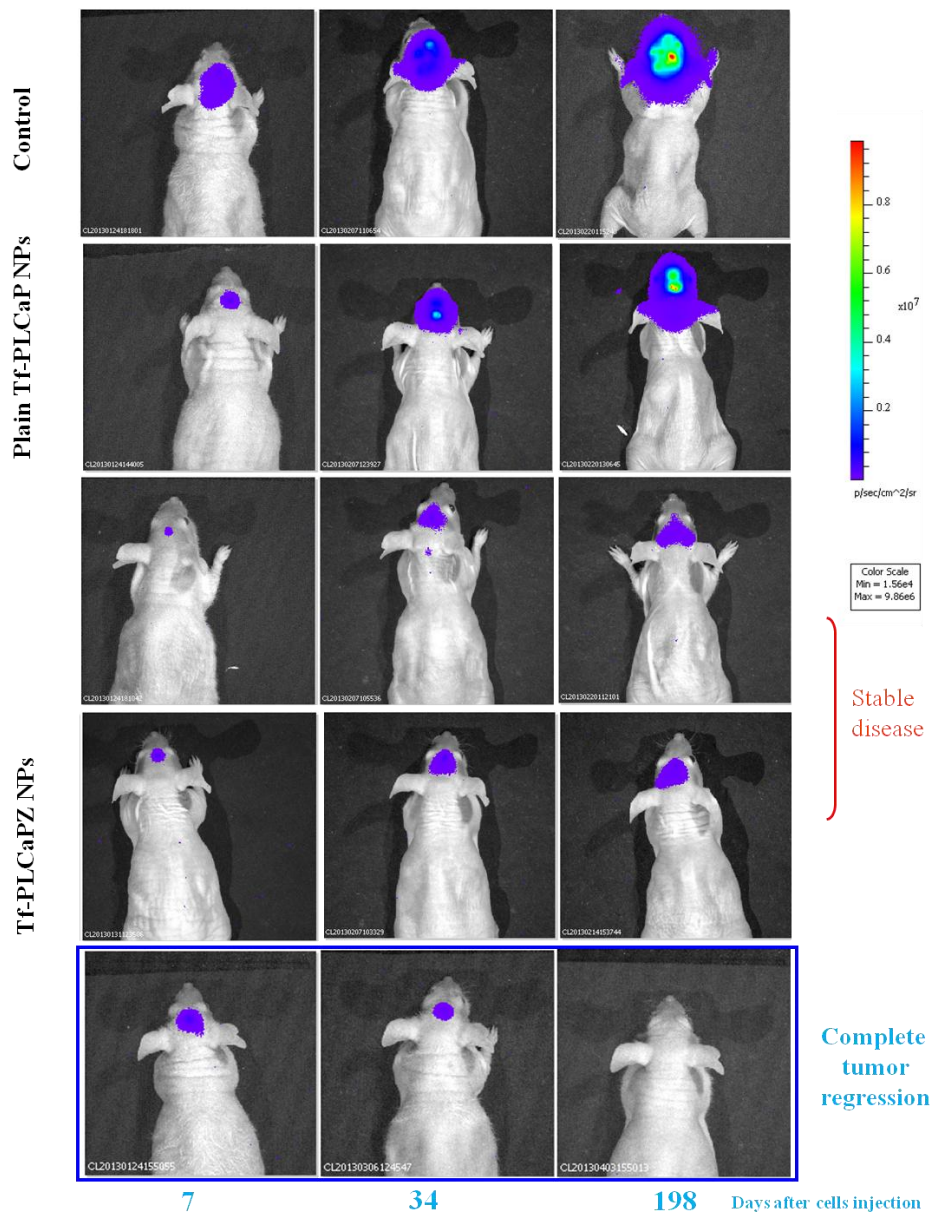


Figure 9. Anti-cancer activity of Tf-PLCaPZ NPs in an orthotopic model of GBM.

Overall, our results clearly demonstrate the therapeutic efficacy of PLCaPZ NPs functionalized with Tf against experimental models of human GBM even on orthotopic tumors that closely mimics the clinical setting.

Discussion

In the present study, we have proposed a new strategy to inhibit GBM cells growth. In a previous work, we demonstrated that self-assembled NPs could be used to successfully deliver ZOL in different cell lines, with a strong potentiation of its anti-cancer effect (Salzano G. *et al.*, 2011). These effects were then confirmed *in vivo* in an experimental model of prostate cancer (Marra M. *et al.*, 2012). On the basis of these interesting results, it should be attractive to use this technology for the delivery of ZOL also in tumors as GBM that, at the moment, are very difficult to treat, also *in vitro*. To this aim, earlier developed self-assembled NPs have been potentiated in order to target TfR, which is overexpressed in different cancer cells, such as GBM. Tf has been successfully used for active targeting of cancer cells and Tf-modified NPs are at the moment in clinical trials (Daniels T.R. *et al.*, 2012). The biological significance of Tf peptide and its receptor has been thoroughly characterized and its relevance when applied to targeting strategies has been widely reported (Daniels T.R. *et al.*, 2012). It has been found a direct correlation between increased expression of Tf receptor and the levels of malignancy in a wide range of tumors, including glioma (Recht L. *et al.*, 1990). In addition, Tf is the major peptide involved in the transportation of iron from the blood into the brain (Burdo J.R. *et al.*, 2003). All this knowledge about the physiological function and expression of Tf and its role in drug delivery provides rationale for the development of Tf-targeted NPs to improve the delivery of a promising anti-cancer agents, such as ZOL, in GBM cells.

The first task of this work consisted in modifying with Tf the surface of the self-assembling NPs, previously developed by our group, sparing their

self-assembling characteristics. This propriety should allow the formation of these NPs easily before use, thus avoiding stability and scale-up.

Therefore, the first step of the work was to change the preparation protocol to conjugate Tf on the surface of the NPs without altering their physical characteristics. The inclusion of Tf in the protocol and in particular the Tf mixing with PEGylated cationic liposomes before complexation with CaPZ, did not result in a significant change in terms of mean diameter, P.I. and ZOL encapsulation efficiency (Table I). Tf complexation with PEGylated cationic liposomes resulted in a strong decrease of the ζ , thus indicating efficient charge shielding, reasonably due to the presence of Tf on the vesicle surface (Table I). Then, in order to determine if the surface modification could influence the hemolytic potential of the Tf-modified NPs, the erythrocytes activity was evaluated in human blood samples using a previously reported method slightly modified (Chen C. *et al.*, 2008). The instability of therapeutic NPs in the blood is considered to be one of the serious limitations in their clinical use. In particular, carrier based on cationic lipids often present hemolytic activity at certain concentrations (Hägerstrand H. *et al.*, 2001). Here, we have investigated if the presence of cationic lipids in the developed NPs can led to an erythrocyte toxicity. Our results revealed that, at the concentration used in the *in vitro* studies, non-targeted PLCaPZ NPs showed a limited hemolytic activity (of ~ 5%). The presence of PEG chain in the NPs formulation could contribute to the low hemolytic activity of these NPs, probably due to a shielding effect on the surface positive charge (Kainthan R.K. *et al.*, 2006). Interestingly, Tf-PLCaPZ NPs showed almost no hemolytic activity, since, according to ASTM F 756–08 a hemolytic

activity less than 2% is generally regarded to a non-toxic effect level (ASTM F-756, 2009) (Figure 1). Since Tf possesses a net negative charge, its introduction on the surface of the NPs reduced significantly the rate of hemolysis compared to no-targeted PLCaPZ NPs (~1% versus ~5%, respectively). Therefore, the significant low rate of hemolysis ($p < 0.001$) observed by using Tf-PLCaPZ NPs can be correlated to the ability of Tf to shield more efficiently the positive charge of the NPs. In addition, the use of a physiological molecule, such as Tf, could further contribute to a biocompatibility of these NPs.

Consequently, we evaluated the effect of NPs functionalization in GBM cell lines. First of all, we evaluated if the GBM cells expressed significant levels of TfR by Western blot analysis. Our results showed that all the three GBM cell lines expressed TfR, with the highest levels in LN229 cells (Figure 2). Interestingly, in LN229 cells, we observed a significant uptake of Tf-PLCaPZ NPs, visualized by confocal microscopy and FACS analysis, suggesting a correlation between the higher levels of Tf in this cell line and the cell internalization of Tf-PLCaPZ NPs. Moreover, if compared to no targeted PLCaPZ NPs, the cell uptake of Tf-PLCaPZ NP was significantly enhanced (Figure 3).

Moreover, Tf-PLCaPZ NPs were able to induce morphological changes in LN229 cells. In particular, Tf-PLCaPZ NPs elicited a significant cell elongation that was much higher than the one induced by free ZOL or by PLCaPZ NPs (Figure 4). To evaluate the biological mechanisms on the basis of the morphological change in LN229 cells, we analyzed in the treated cells, the levels of two differentiation markers, Olig2 and GFAP. GBM is an anaplastic brain tumor characterized by poorly differentiated

neoplastic cells (Sampetrean O. *et al.*, 2013) and it is highly refractory to conventional modalities of treatment. It has been found a direct correlation between the levels of Olig2 and GFAP and the response to chemotherapeutic agents. In particular, glial tumors characterized by high levels of Olig2 and low levels of GFAP (Olig2⁺/GFAP⁻), a condition usually found in oligodendroglioma, are characterized by better prognosis, higher chemosensitivity and better survival (Mokhtari K. *et al.*, 2005). Interestingly, we found that, Tf-PLCaPZ NPs treated LN229 cells expressed higher levels of Olig2 rather than GFAP as compared with free ZOL or PLCaPZ NPs (Figure 4). These results suggest that the treatment with Tf-PLCaPZ NPs could induce an oligodendrocytic differentiation of the LN229 GBM cells.

In a second phase of the study, we investigated the possibility to combine Tf-PLCaPZ NPs with a chemotherapeutic agent, TMZ. TMZ is currently the first line of choice for the treatment of GBM, together with radiotherapy. However, its effectiveness is often limited and it seems to act above all as radiosensitizers in the classical Stupp schedule that represents the gold standard in the treatment of GBM in the first line of treatment while fotemustine is used in the second line (Addeo R. *et al.*, 2009).

In our preliminary study, we found that the treatment of GBM cells with free TMZ was characterized by an *in vitro* refractoriness to TMZ (Table II). On the contrary, the treatment with free ZOL or ZOL incorporated in either PLCaPZ NPs or Tf-PLCaPZ NPs induced a more potent effect on the growth inhibition of GBM cells if compared to TMZ (Table III). In order to investigate if the treatment with NP formulations containing ZOL could sensitize GBM cells to TMZ, synergistic studies were performed.

Previously, it has been reported a synergistic effect of ZOL in combination with conventional cytotoxic drugs (doxorubicin or docetaxel) in particular when these were added to either breast cancer cells or prostate cancer cells before ZOL (Facchini G. *et al.*, 2010). Here, we have studied the synergistic effect of ZOL and TMZ in different sequences of administration. In all the GBM cells, we found a synergistic effect when ZOL was added after TMZ (Figure 6). On the other hand, the concomitant treatment of ZOL and TMZ did not result in a substantial synergism (data not shown). It is worth to note that in all the cases, the treatment of GBM cells with ZOL-containing NPs potentiated the synergistic effect (Table IV). Tf-PLCaPZ NPs appeared to be more active when administered in combination with TMZ on LN-229 cells that express higher levels of TfR. These results suggest that the high expression of TfR may improve the binding and the subsequent internalization of Tf-functionalized NPs and consequently potentiate the antitumor activity of ZOL. It is also interesting to note that, only when using Tf-PLCaPZ NPs, even in the reverse order of administration of TMZ, is possible to find a strong synergism on LN-229 cells (Figure 6).

Finally, we investigated the ability of the Tf-PLCaPZ NPs to overcome the BBB and their consequent efficacy on the inhibition of the tumor growth in an orthotopic model of GBM. Interestingly, we found a marked therapeutic efficacy of Tf-PLCaPZ NPs since, in mice treated with this formulation, a stabilization of the disease and a complete response with regression of tumor was observed (Figure 9).

Conclusions

We have proposed a new strategy to efficiently use ZOL for the treatment of GBM. The developed Tf-PLCaPZ NPs allows for both easy upgrade of the NPs with specific ligands and high ZOL incorporation. The Tf-targeted NPs showed high colloidal stability and small particle sizes. The Tf-PLCaPZ NPs were able to efficiently accumulate into LN229 GBM cells and to consequently inhibit their growth. In addition, the treatment with Tf-PLCaPZ NPs mediated a potent sensitization of GBM cells to non-effective doses of TMZ. Moreover, the functionalization of NPs with Tf was able to increase the anti-tumor activity of ZOL *in vivo*, in a GBM orthotropic model. The successful pharmacological effect on mice, which resulted in a stabilization of the tumor in all the treated animals and in a complete regression of the tumor in a significant percentage of treated animals, opens a new prospective for the future clinical use of ZOL in treatment of brain tumors.

Chapter 2

“Multifunctional polymeric micelles for the co-delivery of an anti-survivin siRNA and paclitaxel for the reversal of drug resistance in ovarian cancer”

Summary

Small interfering RNA (siRNA) are double stranded RNA-based oligonucleotide with the possibility to specifically inhibit a target protein. This potential represent a powerful therapeutic opportunity to treat different form of cancer, among them also form of multiresistant cancer, such as ovarian cancer. This is the second most common gynecological malignancy worldwide. Its current therapy is based on cytoreductive surgery followed by platinum and taxane-based combination chemotherapy. However, after an unpredictable time of response to therapy, a high percentage of patients undergo to a resistant phase. The discovery that survivin, a small anti-apoptotic protein, is involved in chemoresistance, opens a new scenario to overcome multidrug resistance (MDR) in cancer, since siRNA could be used to inhibit the expression of survivin in cancer cells. Interestingly, it has been found that the down-regulation of survivin by siRNA sensitizes cancer cells to chemotherapeutic agents, such as paclitaxel (PXL). However, the clinical use of siRNA is still hampered by an unfavorable pharmacokinetic profile. To address this problem, we developed a novel system to stabilize and deliver siRNA into cancer cells. Namely, we reversibly modified an anti-survivin siRNA with a phosphothioethanol (PE) portion via a reducible disulfide bond and incorporated the resulting siRNA-S-S-PE conjugate into nanosized polyethyleneglycol2000-phosphatidyl ethanolamine (PEG₂₀₀₀-PE)-based polymeric micelles (PM), obtaining the so-called survivin siRNA PM. The activity of these nanopreparations was evaluated in different cancer cell lines by survivin protein down-regulation, tumor cell growth inhibition, and chemosensitization of the treated tumor cells to paclitaxel (PXL). In all the

survivin siRNA PM treated cells, we found a significant decrease of cell viability and down-regulation of survivin protein levels. In addition, the down-regulation of survivin by treating cells with survivin siRNA PM, elicited a significant sensitization of the cells to PXL, in both sensitive and resistant cancer cell lines. In a second phase of the project, we investigated the possibility to co-incorporate anti-survivin siRNA and PXL in the same PM for combined therapy. To this purpose, we developed PMs co-loaded with PXL and anti-survivin siRNA, the so-called survivin siRNA/PXL PM. These multifunctional PMs were prepared by a method very easy to reproduce. The activity of the combination was evaluated *in vitro* on a PXL-resistant ovarian cancer cell lines, SKOV3-tr. We demonstrated successful co-delivery of PXL and survivin siRNA in the same PMs leading to superior therapeutic activity compared to their sequential administration. Finally, to confirm the encouraging *in vitro* results, the antitumor efficiency of the developed multifunctional PM was evaluated in an animal model of SKOV3-tr. Changes in survivin expression, therapeutic efficacy and biological effects of the multifunctional PM, were investigated. Interestingly, the results on xenografted SKOV3-tr mice, revealed a significant down-regulation of survivin expression in tumor tissues together with a potent anticancer activity by using survivin siRNA/PXL PM. In the same model, tumor growth was unaffected when using free PXL. These results demonstrated that survivin siRNA/PXL-co-loaded PM elicited a significant inhibition of the tumor growth of a human xenograft model of SKOV3-tr in mice and encourage the future pre-clinical development of survivin siRNA/PXL PM for the treatment of this and other chemo-resistant tumors.

Introduction

Survivin, the smallest member of the inhibitors of apoptosis (IAP) family, has gained much attention in recent years as a promising new target in cancer therapy due to its differential expression in tumors compared to normal tissues (Ambrosini G. *et al.*, 1997). Survivin plays an important role in the negative regulation of apoptosis as well as in cell division (Altieri D.C., 2003; Yang D. *et al.*, 2004). Moreover, survivin expression in malignant tissues has been correlated with drug resistance (Lu J. *et al.*, 2009). Accordingly, inhibition of survivin has been of clear interest for cancer therapy. In the last years, many researchers have proposed various ways to counteract survivin activity in cancer cells with the aim to inhibit the tumor growth potential and to sensitize the tumor cells to chemotherapeutic agents. RNA interference (RNAi), a cellular post-transcriptional gene silencing mechanism, offers an attractive and powerful approach to efficiently inhibit survivin expression in cancer cells (Fire A. *et al.*, 1998). RNAi can be induced by double-stranded small interfering RNA (siRNA) consisting of 21-25 nucleotides that degrades a target mRNA in a highly sequence specific manner (McManus M.T. *et al.*, 2002; Hannon G.J. *et al.*, 2004; Caplen N.J. *et al.*, 2001). Carvalho A. *et al.* (2003) were the first to use siRNA to suppress survivin levels in HeLa cells, showing a specific depletion of survivin for at least 60 h after the transfection with a specific siRNA. Seth *et al.* have demonstrated the *in vivo* silencing of survivin and a significant dose-dependent decrease of tumor volumes after intravesical instillation of liposomes containing survivin siRNA in an animal model of bladder cancer (Seth S. *et al.*, 2011).

Despite all the potential of siRNA in cancer treatment, selective inhibition of an over-expressed gene via RNAi requires an effective delivery strategy that ameliorates the significant issues associated with its pharmacokinetic profile. In particular, the poor stability in biological fluids and the low cellular uptake impaired siRNA direct use in clinical trials. In the literature, a wide number of non-viral delivery carriers, including liposomes (Zimmerman T.S. *et al.*, 2006; Landen C.N. *et al.*, 2005), lipids (Santel A. *et al.*, 2006; Yano J. *et al.*, 2004), polymers (Kim S.H. *et al.*, 2006; Urban-Klein B. *et al.*, 2005), peptides (Mok H. *et al.*, 2008), virus-based vectors (Grimm D. *et al.*, 2006), and pressurized hydrodynamic injection (Song E. *et al.*, 2003), have been suggested for improved intracellular delivery of siRNA. However, only few have demonstrated clinical applicability due to toxicity and poor stability in biological fluids. Recently, it has been reported that direct conjugation of small drug molecules, aptamers, lipids, peptides, proteins, or polymers to siRNA could improve *in vivo* pharmacokinetic behavior of siRNA, prolong its half-life, and increase its delivery efficiency (Nishina K. *et al.*, 2008; Chu T.C. *et al.*, 2006; Kim S.H. *et al.*, 2006; Lorenz C. *et al.*, 2004; Moschos S.A. *et al.*, 2007; Muratovska A. *et al.*, 2004; Soutschek J. *et al.*, 2004). However, chemical modification of siRNA can affect its activity and specificity, and in such conjugates, siRNA still remains open for degradation by nucleases. Therefore, the transition of siRNA-based approach to the clinical setting requires the development of a suitable delivery system which thoroughly protects siRNA from degradation *in vivo* and at the same time is capable of releasing free siRNA when inside cell. With this in mind, the research group led by Dr. Torchilin V.P. have designed a novel “reversible” siRNA

by attaching siRNA to the phospholipid (PE) via a disulfide linkage, the so-called siRNA-S-S-PE conjugate (Figure 1), (Musacchio T. *et al.*, 2010).

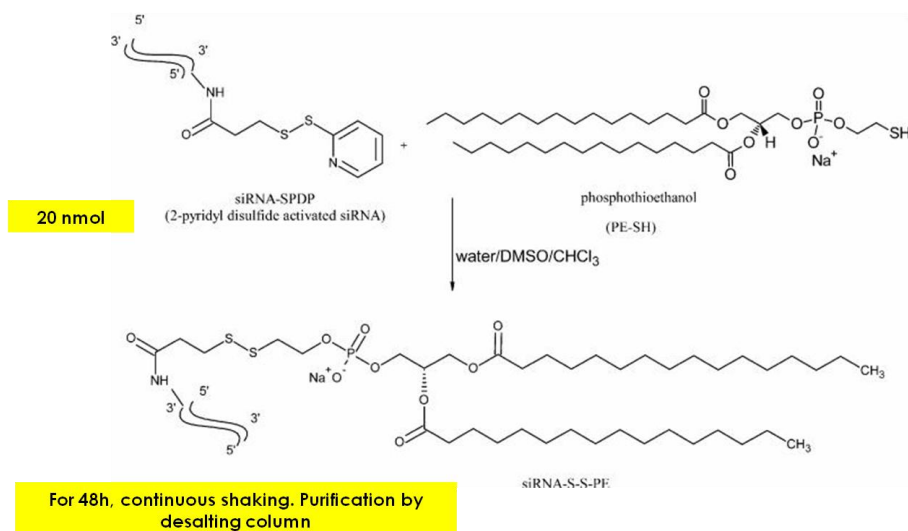


Figure 1. Schematic representation of siRNA-S-S-PE synthesis.

This strategy is based on the high concentration of reductases in the tumor microenvironment over normal tissues (Balendiran G.K. *et al.*, 2004) as well as glutathione inside cancer cells (Estrela J.M. *et al.*, 2006). In particular, when inside the cell, the S-S linkage in a such conjugate will be reduced by the high intracellular glutathione (GSH) and liberate the native siRNA into the cytoplasm. Then, to further protect siRNA-S-S-PE from the nucleolytic degradation on its route to the target, the siRNA-S-S-PE conjugate was incorporated via its hydrophobic PE moiety, into PEG₂₀₀₀-PE-based stable polymeric micelles known to have high stability, prolonged circulation, and accumulation in the areas with an abnormal vascularization, i.e. tumors, via the enhanced permeability and retention (EPR) effect in pathological areas *in vivo* (Sawant R.R. *et al.*, 2010). Such micelles can be also modified to target specific cells (Sawant R.R. *et al.*, 2010). Therefore, the chemical conjugation of siRNA and its incorporation

as conjugate into PM offers the dual advantage of protecting the siRNA from degradation *in vitro* and at the same time, the cleavable disulfide bonds linked to the siRNA, allows to liberate it as free when inside the cell for target-specific gene silencing (Musacchio T. *et al.*, 2010).

Here, we formulated nanosized PEG₂₀₀₀-PE PM for anti-survivin siRNA delivery (Salzano G. *et al.*, 2014). In particular, we developed easy-to-obtain PM through self-assembly of amphiphilic block of PEG₂₀₀₀-PE polymers in an aqueous environment containing preformed survivin siRNA-S-S-PE conjugate. The technological parameters have been optimized in order to obtain PM that can be prepared immediately before use overcoming problems of stability during the storage of many colloidal systems, such as liposomes (Torchilin V.P. *et al.*, 2003). In fact, the developed PM can be prepared offhand by mixing at room temperature preformed polymeric film of PEG₂₀₀₀-PE with a dispersion containing anti-survivin siRNA-S-S-PE conjugate. After few minutes of simple mixing the formulation is ready to be injected. Then, the size characteristics of the PMs, the incorporation efficiency of survivin siRNA, the stability of the siRNA against nuclease and the capability of the disulfide linkage to be cleavage in reducing conditions, were investigated. In a second step, the activity of the developed survivin siRNA PMs was evaluated *in vitro* by measuring the survivin protein levels and cytotoxic effect in different cancer cell lines. *In vitro* cytotoxicity and survivin protein levels assays revealed the ability of survivin siRNA PMs to efficiently inhibit the cell growth and to down-regulate the survivin in different cancer cell lines.

In a second phase of the project, we investigated the potential of combining anti-survivin siRNA and a chemotherapeutic agents, PXL,

within one multifunctional nano-assembly; the aim was to achieve a synergistic effect of the two agents for the treatment of aggressive ovarian cancer. PXL exhibits its anticancer activity by promoting tubulin polymerization and stabilizing microtubules, which results in mitotic G₂/M arrest and apoptosis (Gallagher Jr. B.M. *et al.*, 2007). The clinical effectiveness of PXL, an agent widely used in clinic for the treatment of several tumors, such as ovarian cancer, is often hampered by acquired drug resistance (Singla A.K., *et al.*, 2002). Since sensitization to PXL by survivin down-regulation has been reported (Shen J. *et al.*, 2012; Shen J. *et al.*, 2013; Hu Q. *et al.*, 2012), we evaluated co-treatments with PXL and anti-survivin siRNA. The over-expression of survivin has been associated with poor prognosis and aggressiveness of the tumors (Salz W. *et al.*, 2005). In advanced ovarian carcinomas, it has been found that forced expression of survivin are directly correlated with a clinical resistance to taxane chemotherapy (Zaffaroni N. *et al.*, 2002).

To this purpose, we upgraded the developed PM by co-encapsulating anti-survivin siRNA and PXL in the same PM. The so-called survivin siRNA/PXL PM showed optimal technological characteristics, highlighting the ability of the PM to efficiently co-encapsulate chemotherapeutic agents and siRNA for multifunctional therapy. Then, we investigated the therapeutic potential of the developed multifunctional PM, namely survivin siRNA/PXL PM, especially concerning the anti-cancer activity in a xenografts model of PXL-resistant ovarian carcinoma, SKOV3-tr. Moreover, the gene silencing and the biochemical effects of the formulation were studied on tumors collected from animals after the treatment.

Materials and Methods

Materials

Unless otherwise stated all chemicals were from Sigma-Aldrich (Saint Louis, MO, USA). Survivin siRNA with the following sense sequence 5'-GCAUUCGUCCGGUUGCGCUdTdT-3' and a scrambled siRNA with the following sense sequence 5'-AUGAACUUCAGGGUCAGCUdTdT-3' have been used. Both siRNAs modified at the 3'-end of the sense strand with N-succinimidyl 3-(2-pyridyldithio)propionate (SPDP) group were purchased from Thermo Scientific Dharmacon (Pittsburgh PA, USA). The paclitaxel (PXL) was purchased from LC Laboratories (Woburn MA, United States). The Paclitaxel Oregon green (P22310) was from Invitrogen, CA. The 1,2-dipalmitoyl-sn-glycero-3-phosphothioethanol (PE-SH, MW 731) and 1,2-distearoyl-sn-glycero-3-phosphoethanolamine-N-[methoxy(poly(ethyleneglycol))-2000](PEG₂₀₀₀-PE) were from Avanti Polar Lipids (Alabaster, AL). The d-Salt dextran desalting column was from Pierce (Rockford, IL, USA). The human total survivin immunoassay, Surveyor IC, was purchased from R&D System (Minneapolis, MN). RNase/DNase-free water was obtained from MP Biomedicals (Solon, OH), the phosphate saline buffer (PBS) 10× solution and bovine serum albumin (Fraction V) were from Fisher Scientific (Fair Lawn, NJ). β -tubulin antibody (G-8) was from Santa Cruz Biotechnology (Dallas, Texas, USA). Fluorescein (FITC)-conjugated AffiniPure Donkey Anti-Mouse IgG (H+L) was provided by Jackson ImmunoResearch Laboratories, Inc. (West Grove, PA). Hoechst 33342 trihydrochloride, trihydrate, was purchased from Molecular Probes (Eugene, Oregon, USA). Vecta Shield mounting medium for fluorescence, H-1000, was from Vector Laboratories, Inc. (Burlingame,

CA, USA). The RNeasy kit for mRNA isolation was obtained from Qiagen (Germantown, MD, USA). The First Strand cDNA synthesis kit and the SYBR green kit for qRT-PCR were purchased from Roche, USA. Primers for the survivin gene (5'CTGCCTGGCAGCCCTTT-3') and (5'CCTCCAGAAGGGCCA-3') and for β -actin were obtained from Invitrogen, CA. The Aspartate aminotransferase (AST)/Alanine aminotransferase (ALT) assay kit was purchased from the biomedical research service center at SUNY Buffalo (Buffalo, NY, USA). The rabbit anti-survivin antibody, AF886, was obtained from R&D System (Minneapolis, MN, USA). Texas red-x goat anti-rabbit IgG (T6391) and Alexa Fluor 488 goat anti-mouse IgG, IgA, IgM (H+L) were provided by Life Technologies (Eugene, Oregon, USA). FragEL DNA fragmentation detection kit fluorescent TdT enzyme was provided by EMD Chemicals, Inc (San Diego, CA, USA).

Cell Culture

Human ovarian cancer cell line (A2780) and human breast cancer cell line (MDA-MB231) were cultured in DMEM medium, containing 10% fetal bovine serum (FBS), 100 U/mL penicillin G sodium and 100 mg/mL streptomycin sulfate (complete medium), in a humidified atmosphere of 95% air 5% CO₂ at 37 °C. Human ovarian cancer cell line sensitive (SKOV3) and multi drug resistant (MDR) (SKOV3-tr) were grown in the complete RPMI 1640 medium. The SKOV3-tr cells have been widely characterized and are known to overexpress the MDR-1 gene (Duan Z. *et al.*, 1999). All the cell lines were obtained from the American Type Culture Collection (ATCC, Manassas, VA, USA). Trypan Blue solution and trypsin were from CellGro (Kansas City, MO, USA).

Synthesis of survivin siRNA-S-S-PE Conjugate

The survivin siRNA-S-S-PE conjugate was synthesized as previously described (Musacchio T. *et al.* 2010). Briefly, an aqueous solution of the SPDP-activated siRNA (20 nmol in 120 μ L of RNase/DNase-free water), was added dropwise to a solution of PE-SH (2 μ mol) in DMSO and CHCl_3 (total volume of organic solvents 350 μ L). The reaction was carried out for 48 h at room temperature with continuous stirring. The un-reacted reagents were removed by desalting column. The collected samples containing the survivin siRNA-S-S-PE conjugate were freeze-dried for overnight. After freeze-drying, the survivin siRNA-S-S-PE conjugate was hydrated with PBS pH 7.4 at a final siRNA concentration of 20 nmol/ml and ultracentrifuged for 1 min at 14.5×1000 rpm to further remove mixed solvents and/or PE-SH. The survivin siRNA-S-S-PE conjugate was stored at -20 °C. The conjugation efficiency and the amount of survivin siRNA-S-S-PE conjugate was determined, after purification, by absorbance at 260 nm using a Nanodrop (2000c Spectrophotometers, Thermo Scientific). Scrambled siRNA was modified following the same protocol.

Incorporation of siRNA-S-S-PE in PEG₂₀₀₀-PE Micelles

The PEG₂₀₀₀-PE micelles containing siRNA-S-S-PE were prepared by hydration of a thin polymeric film (Salzano G. *et al.*, 2014) . In particular, PEG₂₀₀₀-PE was dissolved in chloroform (20 mg/ml) and the resulting solution was added to a 50 ml round-bottom flask. The organic solvent was removed under reduced pressure by a rotary evaporator under nitrogen atmosphere, followed by freeze-drying. Then, the polymeric film was hydrated with 1 ml of survivin siRNA-S-S-PE in phosphate buffer at pH

7.4 at different PEG₂₀₀₀-PE/siRNA-S-S-PE weight ratio (1:200, 1:500, 1:750). The resulting dispersion was gently vortexed to form mixed micelles, so-called survivin siRNA PM. PEG₂₀₀₀-PE-based PM containing scrambled siRNA-S-S-PE and plain PM were prepared similarly. Each formulation was prepared in triplicate.

Preparation and characterization of multifunctional PM co-encapsulating survivin siRNA and PXL

PXL was incorporated in survivin siRNA PM as follow. Briefly, an organic solution of PXL in methanol (1 mg/mL) was added to the PEG₂₀₀₀-PE mixture in chloroform. The initial loading of PXL into micelles was 1% w/w. The incorporation of survivin siRNA-S-S-PE into these micelles was determined as reported above. The encapsulation efficiency of PXL in PM was determined as previously reported (Musacchio T. *et al.*, 2010). For imaging studies survivin siRNA/PXL PM contained 0.1% (w/w) of Oregon Green labeled PXL were prepared similarly.

Characterization of PM

The mean diameter of PM containing survivin siRNA-S-S-PE alone or in combination with PXL, was determined at 20°C by the dynamic light scattering (DLS) using a Zeta Plus Instrument (Brookhaven Instrument Co., Holtsville, NY, USA). Briefly, each sample was diluted in deionizer/filtered water and analyzed with detector at 90° angle. As a measure of the particle size distribution, polydispersity index (P.I.) was used. For each batch, mean diameter and size distribution were the mean of three measures. For each formulation, the mean diameter and P.I. were calculated as the mean of three different batches.

Incorporation of siRNA-S-S-PE Conjugate in PEG₂₀₀₀-PE PM

The quantitative analysis of siRNA-S-S-PE in PM was performed by the size-exclusion high-performance liquid chromatography (SEC-HPLC). For the analysis, the HPLC system (D-7000 HPLC, Hitachi, Japan) equipped with a Shodex protein KW-804 column (Showa Denko, Japan) and an UV detection at 280 nm, was used. The mobile phase was composed of 50 mM NaCl and 50 mM Tris-HCl (pH 8.0) and the flow rate at 1.0 mL/min. The siRNA-S-S-PE loading efficiency into PM was evaluated by ratio of the area under the peaks at the same retention time (*t_r* ca. 10 min) of survivin siRNA-S-S-PE not encapsulated in PM and the survivin siRNA-S-S-PE initially added to the PM. As a control, plain PM were also analyzed. To confirm the data collected by SEC-HPLC, we analyzed the same samples also by the reverse phase HPLC (RP-HPLC). The RP-HPLC analysis was carried out as previously reported (Musacchio T., *et al.*, 2010). Then, we evaluated the loading efficiency of PXL in survivin siRNA PM. The quantitative analysis of PXL was determined by RP-HPLC as previously reported (Musacchio T. *et al.*, 2009), using a XBridge column (4.6mm×250mm, Waters, Milliford, USA). The mobile phase consisted of water and acetonitrile with volume ratio 60:40, the elution was performed at a rate of 1.0 ml/min, and PXL was detected from injected sample (50µL) at 227nm.

Cell viability assay

A2780, MDA-MB 231, SKOV3 and SKOV3-tr cells were seeded at a density of 3×10^3 cells/well in 96-well culture plates for 24 h. After 24 h, the cells were treated with various concentrations of survivin siRNA-S-S-

PE free or in PM, scrambled siRNA-S-S-PE in PM and plain PM, in serum-containing media. The final concentration of siRNA-S-S-PE was in the range of 200 to 17.6 nM. After 6 h, the medium was replaced with fresh medium, and the cells were incubated until the 48-hour-time point was reached. Cells without treatment were used as control. The cell viability was determined by Cell Titer Blue assay following manufacturer's protocol. The experiments were done in triplicate on three different sample preparations.

Survivin Protein Assay

A2780, MDA-MB231, SKOV3 and SKOV3-tr cells ($3 \cdot 10^4$ cells per well) were seeded into 48-well plates. Cells were treated with survivin siRNA PM at a final concentration of 200 nM in serum-containing medium for 6 h. Cells were washed once with fresh medium and maintained in fresh medium until 48 h. Cells were rinsed three times with PBS and treated with 200 μ l of cold lysis buffer for 30 minutes on ice (R&D system). Cell lysates were collected, vortexed, and incubated on ice for other 15 minutes twice. Cell debris was removed by centrifugation at 2000g for 5 min, and protein concentrations were determined by BCA assay after 6-fold dilution in PBS. Samples were added into captured antibody pre-coated 96-well plates, and human survivin was assayed by ELISA after 6-fold dilution in assay buffer (R&D system).

Chemosensitization Study

MDA-MB231, SKOV3 and SKOV3-tr cells ($3 \cdot 10^3$ per well) were seeded into 96-well plates. Cells were treated with survivin siRNA PM at the concentration of 200 nM for 6 h. After 6 h, the medium was replaced with

fresh medium, and the cells were incubated for another 48 h. Cells were then exposed to different concentrations of PXL for 24 h. Cell viability was detected by the Cell Titer Blue assay.

Immunohistochemical staining

SKOV3-tr cells ($2 \cdot 10^4$ per coverslip) were seeded and grown on glass coverslips coated with 1% gelatin cross-linked with 0.5% glutaraldehyde in a 12-well plate. After 24 h, cells were treated with 200 nM of survivin siRNA PM for 6 h. After 6 h, the medium was replaced with fresh medium, and the cells were incubated for another 48 h. Then, cells were exposed to 40 nM of free PXL for 24 h. As controls, free PXL (40 nM), survivin siRNA PM, and untreated cells were used. Cells were washed three times with PBS and then were fixed with 4% paraformaldehyde. Fixed cells were made permeable with 0.2% Triton X-100 in PBS and incubated with a monoclonal antibody against β -tubulin (1:10) for 1 h in 1% bovine serum albumin/PBS. After washing, cells were incubated with a secondary FITC-labeled mouse-immunoglobulin G targeting antibody (1:100) for 1 h in 1% bovine serum albumin/PBS. After washing, cells were incubated with Hoechst 33342 (5 μ M) for nuclear staining. The coverslips were mounted on glass slides with Fluoromount-G (Fisher Scientific, Waltham, MA) medium and sealed using a nail lacquer. The slides were observed with a Zeiss LSM 700 inverted confocal microscope (Carl Zeiss Co. Ltd., Jena, Germany) equipped with a 63x, 1.4-numerical aperture plan-apochromat oil-immersion objective. The images were analyzed using the ImageJ version 1.42 software (NIH, Bethesda, MD).

In vitro cytotoxicity of PM co-loaded with the combination of survivin siRNA-S-S-PE and PXL

SKOV3-tr cells ($3 \cdot 10^3$ cells/well) were seeded in 96-well plates. After 24 h the cells were treated with different concentrations of survivin siRNA/PXL PM for 6 h in serum contained media. After 6 h, the medium was replaced with fresh medium, and the cells were incubated for another 72 h. Same concentrations of free PXL, survivin siRNA PM, and scrambled siRNA PM were used as controls. The cell viability was assessed by the Cell Titer Blue assay.

In vivo studies: Cell Culture

Human ovarian adenocarcinoma cell line, MDR SKOV3-tr, was obtained from the American Type Culture Collection (ATCC, Manassas, VA, USA). The cells were grown in RPMI®-1640 medium supplemented with 10% (v/v) fetal bovine serum (FBS), and 100 U/mL penicillin G sodium and 100 mg/mL streptomycin sulfate (complete medium), in a humidified atmosphere of 95% air 5% CO₂ at 37 °C. The SKOV3-tr cells have been widely characterized and are known to over express the MDR-1 gene (Duan Z. *et al.*, 1999). For the subculture, cells growing as monolayer were detached from the tissue flasks by treatment with trypsin/ EDTA. The viability and cell count were monitored routinely using trypan blue dye exclusion method. The cells were harvested during the logarithmic growth phase and re-suspended in serum free medium before inoculation in animals.

Experimental model

The experimental protocol involving use of animals was approved by the Institutional Animal Care and Use Committee of Northeastern University. SCID female nude mice (nu/nu), 6-8 weeks old and weighing 20-25 g were purchased from Charles River Laboratories (Cambridge, MA) and were housed under controlled laboratory conditions in polycarbonate cages. The animals were allowed to acclimate for at least 48 hr before any experiment.

Subcutaneous tumor xenografts development

Approximately, 7 million of SKOV3-tr cells, suspended in 100 μ l of Matrigel® (in free serum media 1:1 volume ratio), were injected subcutaneously into the left flank of mice under light isoflurane anesthesia. Palpable solid tumors developed within 15 days post tumor cell inoculation and as soon as tumor volume reached 150-200 mm³, the animals were randomly allotted to 5 different controls and treatment groups [i.e., PBS, PXL in Cremophore EL1-ethanol (1:1) mixture with normal saline (Taxol), PM containing scrambled siRNA-S-S-PE conjugate and PXL in combination (scrambled siRNA/PXL PM), PM containing survivin siRNA-S-S-PE conjugate (survivin siRNA PM) and PM containing survivin siRNA-S-S-PE and PXL in combination (survivin siRNA/PXL PM)]. Six animals *per* group were used for the experiment. All controls and micelle formulations were diluted and suspended in sterile PBS. Each tumor-bearing animal received siRNA-S-S-PE at a dose of 20 μ g, corresponding to 1mg/kg *per* injection, and PXL at a dose 10 mg/kg both in Cremophore solution or in PM by intravenous administration through the tail vein once *per* week for 5 consecutive weeks.

Evaluation of therapeutic efficacy

The tumor diameters were measured three times weekly with a vernier calipers in 2 dimensions. Individual tumor volumes (V) were calculated using the formula (Tomayko M.M. *et al.*, 1989):

$$V = [\text{length} \times (\text{width})^2]/2$$

where length (L) is the longest diameter and width (W) is the shortest diameter perpendicular to length.

Growth curves for groups of tumors are presented as the Relative Tumor Volume (RTV), defined as V_n/V_0 , where V_n was the tumor volume in mm^3 on day 'n' (V_n) and V_0 at the start of the treatment plotted versus time in days. Mean RTV (mRTV) and standard deviation were calculated per each group. At the end of the experiment, the animals were killed by cervical dislocation and the tumor mass was harvested and weighed.

Evaluation of repeated dose toxicity in mice

For safety evaluation of the controls and survivin siRNA/PXL PM formulation, the body weight of each mouse was determined three times *per* week and related to the first day as percent change in body weight. In addition, blood samples were collected via cardiac puncture before the time of sacrifice and the levels of serum aspartate amino transferase (AST) and alanine amino transferase (ALT) were measured. In particular, the serum was obtained by centrifugation of the freshly collected blood samples at $2,000 \times g$ for 30 min at 4°C . Then, AST and ALT were measured using the manufacturer's standard kinetic assay protocol (Biomedical Research Service).

Collection of Tumor Tissues

Tumors were excised, dissected free of the skin and body tissue and weighed on a digital balance. Then, the tumors were immediately snap-frozen in liquid nitrogen and maintained at -80°C until ready for sectioning. For immunofluorescence analysis, frozen sections (6 µm) were cut on a Cryostats microtome (Thermo Scientific), placed on glass slides and stored at -20°C until they were used.

Tumor cell apoptosis

Tumor sections were stained by Hoechst 33342, and the tumor cell apoptosis was analyzed by terminal deoxynucleotidyl transferase dUTP nick end labeling assay using a FragEL DNA Fragmentation Detection Kit, according to the protocol described by the supplier. The pictures were taken by confocal microscopy. The slides were visualized by light microscopy at 40× magnification.

Evaluation of survivin mRNA expression by using RT-PCR.

Survivin mRNA expression was assayed by performing real-time PCR from different tumor tissues. Tumors were vortexed in a 50mL tube containing 1 mL of cold PBS. Total RNA was isolated from the cells using the RNeasy mini kit (Qiagen) according to the manufacturer's instructions. cDNA was synthesized from 250 ng of total RNA primed with a random hexamer using the Superscript First-Strand System (Invitrogen). For the experiment we used the following survivin primer sequence: human survivin: (forward) 5'-CTGCCTGGCAGCCCTTT-3' and (reverse) 5'-CCTCCAAGAAGGGCCAGTTC-3' (Nakahara T. *et al.*, 2007). Real-time

PCR was done using the ABI Prism 7900 sequence detection system and the SYBR Green PCR Master Mix (Applied Biosystems) according to the manufacturer's instructions. Dissociation curve analyses were done to verify that there was neither unspecific amplification nor formation of primer dimers. Values were calculated based on standard curves generated for each gene. Normalization of samples was determined by dividing copies of survivin transcripts by copies of β -actin. All sets of reactions were conducted in triplicate. The relative expression levels are expressed as a percentage of the indicated control.

Determination of survivin protein expression by immunofluorescence analysis

Survivin immunofluorescence analysis was performed on frozen tumor sections. In detail, tumor sections were fixed with 4% of paraformaldehyde for 20 min at room temperature. After twice washing with PBS, slides were immersed in 0.5 % of H₂O₂/PBS solution at room temperature for 10 min to block endogenous peroxidase activity. The slides were rinsed in PBS solution for two changes, 5 min each, and then, incubated in 1% of Triton X-100 solution for 10 min. Enzymatic activity and non-specific binding sites were blocked by incubating the slides in 10% of FBS for 1 hour at room temperature in a humidified chamber. Subsequently, replicate sections were incubated at 4°C overnight with a primary rabbit anti-survivin antibody (AF886; R&D System) at a final concentration of 10 µg/ml. Thorough rinsing was followed by incubation with red-fluorescent dye-labeled anti-rabbit IgG (10 µg/ml; T6391; Life Technologies) for 1 hour. Negative controls for each tissue section were performed leaving out

the primary antibody. Finally, the nuclei were stained with Hoechst 33342 (5 μ M) for 15 min at room temperature and the stained sections were observed and photographed using a Nikon Eclipse E400 microscope and a Spot Advanced software (Spot Imaging).

Evaluation of the simultaneous intra-tumor accumulation of PXL and down-regulation of survivin expression in tumor sections

For this experiment, mice (n=3) were injected once with survivin siRNA/PXL PM. After 48 hours the animals were injected with survivin siRNA/PXL PM containing Oregon Green labeled PXL (0.1% w/w). After 1 hour the animals were sacrificed. Tumors were excised and processed as above under light protection. At the same time, the intra-tumor accumulation of Oregon Green labeled PXL and survivin protein expression were evaluated. The survivin protein expression was evaluated by immunofluorescence analysis, as reported above. The nuclei were stained with Hoechst 33342. Negative control, such as untreated tumor sections and sections exposed to the secondary antibody only, were processed as described above. Images were recorded by confocal microscopy.

Tubulin immunostaining

Frozen sections were processed as above and incubated with a monoclonal antibody against β -tubulin (G-8; Santa Cruz Biotechnology; dilution 1:50) for overnight at 4°C. After washing, sections were incubated with a secondary Alexa Fluor 488-labeled goat anti-mouse IgG targeting antibody (dilution 1:100) for 1 hour at room temperature. Then, after washing, sections were incubated with Hoechst 33342 (5 μ M) for nuclear staining.

The slides were mounted on glass slides with Fluoromount-G (Fisher Scientific, Waltham, MA) medium and sealed using a nail lacquer. Negative control sections were exposed to the secondary antibody only and processed as described above. The slides were observed with a Zeiss LSM 700 inverted confocal microscope (Carl Zeiss Co. Ltd., Jena, Germany) equipped with a 63x, 1.4-numerical aperture plan-apochromat oil-immersion objective. The images were analyzed using the ImageJ version 1.42.

Statistical analysis

For comparison of several groups, one-way ANOVA for multiple groups, followed by Newman-Keuls test if $P < 0.05$ was performed using GraphPad Prism version 5.0 software (GraphPad Software, Inc, San Diego, CA). All numerical data are expressed as mean \pm SD, $n = 3$ or more, from 3 different experiments. Any p values less than 0.05 was considered statistically significant.

Results

Synthesis and characterization of survivin siRNA PM

In this study, we proposed a new strategy to stabilize and deliver siRNA against survivin into cancer cells. As the first step, we synthesized a survivin siRNA conjugated with a phospholipid (PE-SH) with the disulfide linkage at the 3'-end of the modified siRNA SPDP sense strand. The yield of the conjugation reaction between siRNA and PE was ~90%. Survivin siRNA-S-S-PE conjugate was then incorporated in PM. We have optimized the weight ratio (siRNA conjugate to PEG₂₀₀₀-PE to the micelle-forming component) required to obtain PM with narrow size distribution and high siRNA-S-S-PE incorporation efficiency. More specifically, we prepared PM at a survivin siRNA-S-S-PE/PEG₂₀₀₀-PE weight ratio of 1:200, 1:500 and 1:750, respectively. As reported in Table I, at the ratios tested, the PM were characterized with mean diameter of ~20 nm and a narrow size distribution, with a P.I. ≤ 0.2 .

Formulations (weight ratio)	Mean Diameter (nm \pm SD)	P.I. \pm SD	Survivin siRNA incorporation efficiency (% \pm SD)
Survivin siRNA PM (1:200)	18.7 \pm 3.5	0.191 \pm 0.08	26.0 \pm 5.0
Survivin siRNA PM (1:500)	18.3 \pm 2.0	0.189 \pm 0.06	31.0 \pm 3.8
Survivin siRNA PM (1:750)	21.5 \pm 3.3	0.160 \pm 0.05	52.0 \pm 1.6

Table I. Physical characteristics of survivin siRNA PM.

The incorporation efficiency of survivin siRNA-S-S-PE in PM was determined by SEC-HPLC. After injection of survivin siRNA PM, SEC-HPLC analysis demonstrated that the peak at ca. 8 min corresponded to PM containing survivin siRNA, while the peak at ca. 10 min corresponded to free siRNA-S-S-PE (Figure 2). Plain PM analyzed at the same

concentration as survivin siRNA PM showed the same peak as PM containing survivin siRNA at ca. 8 min. Therefore, we calculated the survivin siRNA incorporation efficiency by the ratio of free survivin siRNA-S-S-PE, not incorporated in PM, and survivin siRNA-S-S-PE initially added to micelle-forming components.

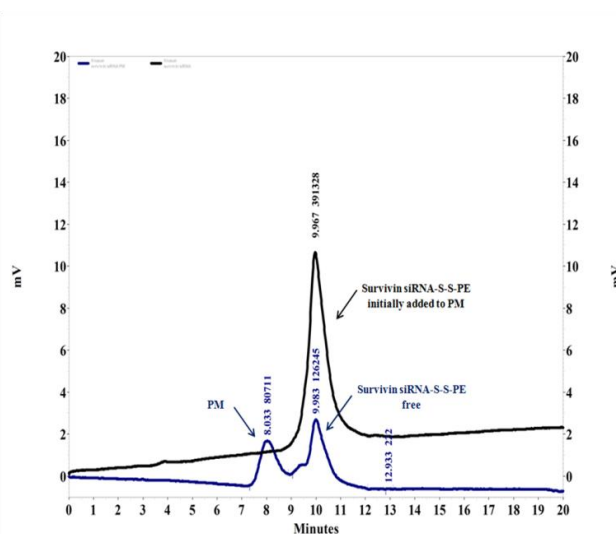


Figure 2. Incorporation efficiency of the modified siRNA into PM determined by SEC. The degree of the incorporation efficiency was measured by ratio of the area under the peak of free survivin siRNA-S-S-PE, not incorporated in PM, and the siRNA-S-S-PE initially added to PM at the same retention time (tr ca. 10 min). As a reference, plain PM were used.

As shown in the Table I, the highest loading efficiency, about 50%, was reached only with PM prepared with the highest amount of polymer, namely with a weight ratio of 1:750. These data were confirmed by RP-HPLC using previously described methods (Salzano G. *et al.*, 2014) (data not shown). This formulation was selected for the subsequent studies.

In the following step, the co-encapsulation of survivin siRNA-S-S-PE and PXL in PM was investigated. In particular, the attention was focused on the

effect of PXL on the physical characteristics of PM, i.e. size and siRNA-S-S-PE loading efficiency. As reported in the Table II, when PXL was added to survivin siRNA PM, no change in the size and in the loading efficiency was observed. In particular, survivin siRNA/PXL PM had a mean diameter of about 22 nm with narrow size distribution (PI< 0.2). Chromatographic analysis of non-encapsulated survivin siRNA-S-S-PE and PXL showed an encapsulation efficiency of about 50% and 70%, respectively.

Formulations	Mean Diameter (nm ± SD)	P.I. ± SD	Survivin siRNA incorporation efficiency (% ± SD)	PXL incorporation efficiency (% ± SD)
Survivin siRNA PM	21.5 ± 3.3	0.160 ± 0.05	50.0 ± 1.0	-
Survivin siRNA/PXL PM	25.0 ± 3.6	0.190 ± 0.07	51.0 ± 1.5	69.9 ± 2.5

Table II. Physical characteristics of PM co-loaded with survivin siRNA-S-S-PE and PXL.

Effect of survivin siRNA PM on the viability of cancer cell lines

The effect of survivin siRNA-S-S-PE incorporated in PM on the growth of different human cancer cell lines, namely breast (MDA-MB231), ovarian (A2780, SKOV3), and paclitaxel-resistant ovarian cell (SKOV3-tr), was investigated by the Cell Titer Blue assay. In the Figure 3, the cell viability (%) after treatment with 200 nM of survivin siRNA-S-S-PE in PM in the different cell lines analyzed after 48 h, is reported. In all sensitive cell lines, when considering survivin siRNA-S-S-PE incorporated in PM, we found a significant ($p < 0.001$ survivin siRNA PM versus the other treatments) anti-proliferative effect. The highest cell growth inhibition was observed in ovarian cancer cells, especially in A2780, reaching a reduction of cell viability of about 70%. No toxicity of PM or micelles prepared with

irrelevant siRNA was observed indicating the effect was mediated by RNAi toxicity, which corresponds to earlier mentioned data (Sawant R.R. *et al.*, 2010). In PXL-resistant SKOV3-tr cells however, no significant reduction of the cell viability was found under the action of siRNA-containing micelles.

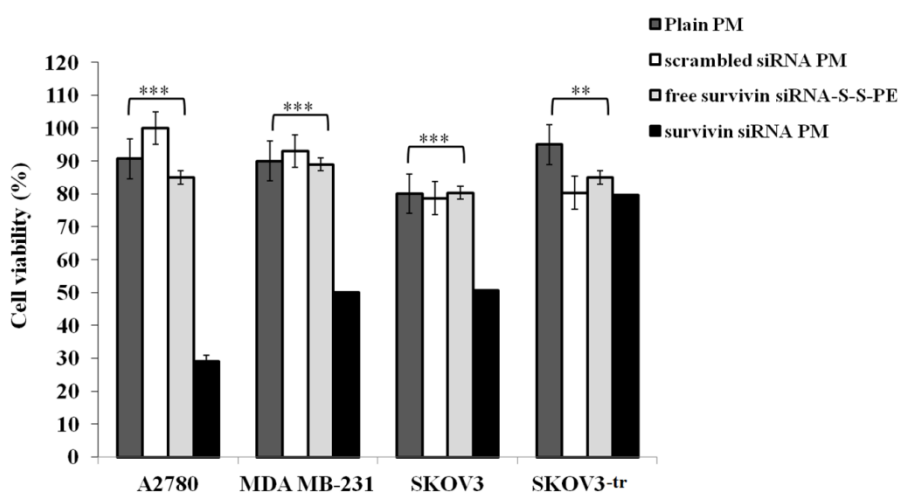


Figure 3. Viability of different cancer cells. Cells were treated with survivin siRNA PM at a final siRNA concentration of 200 nM in the serum-containing medium for 6 h. Cell viability in the presence of survivin siRNA PM, free survivin siRNA-S-S-PE conjugate, PM containing scrambled siRNA-S-S-PE, and plain PM was followed by Cell Titer Blue assay after 48 h of incubation. ** $p < 0.01$, and *** $p < 0.001$ values were obtained by comparing survivin siRNA PM to all the other treatments. Results were obtained from three independent experiments in triplicate ($n = 9$). Mean \pm SD.

Survivin protein levels

Survivin protein levels in the cells treated with survivin siRNA-S-S-PE in PM were then evaluated by ELISA. As illustrated in Figure 4, after treatment with PM containing survivin siRNA-S-S-PE, a significant down-regulation of survivin, by about 30% ($p < 0.01$ survivin siRNA PM versus the other treatments), was observed in all the cell lines. Noteworthy, a significant down-regulation (by about 30%) of survivin levels was observed also in survivin over-expressing SKOV3-tr cells. In cells treated

with free survivin siRNA-S-S-PE, and with PM containing scrambled siRNA-S-S-PE, no significant decrease of survivin level was observed.

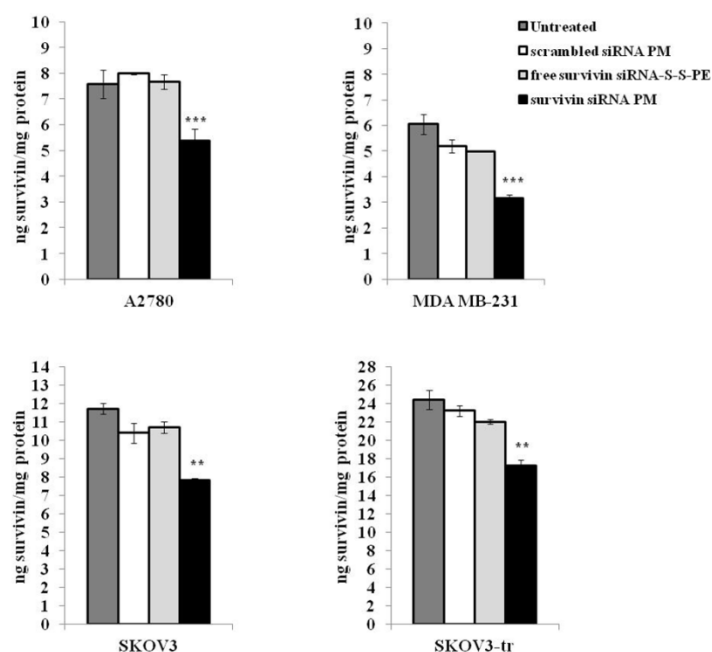


Figure 4. Survivin protein levels in A2780, MDA-MB231, SKOV3, and SKOV3-tr cells after different treatments. Survivin siRNA was quantified 48 h after the treatment by the ELISA method. The data are expressed as ng of survivin protein per mg of protein. Data = mean \pm SD (n = 3). **p < 0.01, and ***p < 0.001 values were obtained by comparing survivin siRNA PM to all the other treatments. Results were obtained from three independent experiments in triplicate (n = 9). Mean \pm SD.

Chemosensitization study

In order to evaluate whether the down-regulation of survivin resulting from the treatment with survivin siRNA PM is able to sensitize cells to PXL, chemosensitization studies were performed. In particular, survivin siRNA PM pre-treated MDA-MB-231, SKOV3 and SKOV3-tr cells were exposed to increasing concentrations of PXL, and the resultant cell viabilities are summarized in Figures 5 a, b and c, respectively. As detailed in Figure 5, in all the cell lines tested, no toxicity was detected with free PXL at a dose range from 40 nM to 3.5 nM after 24 h of treatment. Increasing the

incubation time to 72 h lead to significant toxicity in PXL-sensitive cell lines whereas none was detected in SKOV3-tr, using the same range of concentrations (data not shown). Confirming our initial hypothesis, the down-regulation of survivin by pre-treatment of the cells with survivin siRNA PM, strongly sensitized the cells to PXL. In particular, a significant increase of the PXL cytotoxicity was observed after only 24 h of cell exposure to the drug (Figure 5). These results were confirmed by the immunofluorescence analysis.

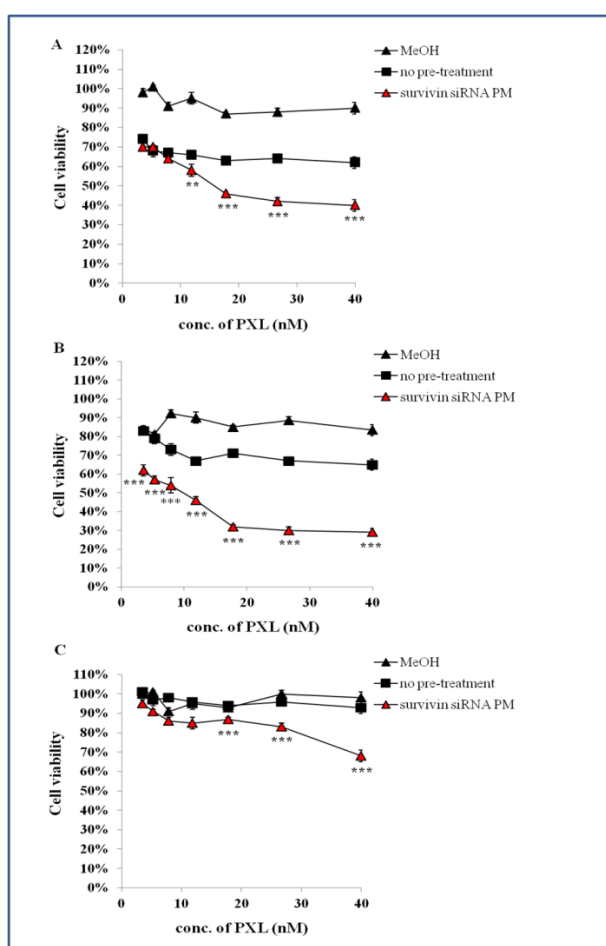


Figure 5. Chemosensitization of MDA MB-231(A), SKOV3 (B), and SKOV3-tr (C) cells mediated by the pre-treatment with survivin siRNA PM. Cells were incubated with survivin siRNA PM (range of siRNA concentrations from 200 to 17.5 nM) for 6 h. Forty eight hours later, cells were challenged with various concentrations of PXL. The viability of cells was measured 24 h later by the CTB assay. Data = mean \pm SD (n

=3).**p < 0.01, and ***p < 0.001 values were obtained by comparing survivin siRNA PM pre-treated cells (survivin siRNA PM) to PXL no pre treated cells (no pre-treatment).

Figure 6 shows the influence of the pre-treatment with survivin siRNA PM on the PXL activity in microtubules stabilization in the resistant cancer cell line, SKOV3-tr. In untreated cells, in cells treated for 24 h with 40 nM of PXL and cells treated with survivin siRNA PM for 48 h (Figure 6 A,B,C, respectively), microtubules appear “healthy” with elongated and fibrillary extensions from around the nucleus to the cell periphery. In contrast, the down regulation of survivin mediated by pre-treatment with survivin siRNA PM for 48 h, sensitize SKOV3-tr cells to PXL action on microtubule organization (Figure 6D). Here, microtubules appear disassembled and characterized by a loss of fibrillar extensions as confirmed by the dense organization of microtubule network around the nucleus. The nuclei begin to fragment, reflective of cell death. These results confirm that survivin down-regulation enhances the PXL activity in microtubule destabilization.

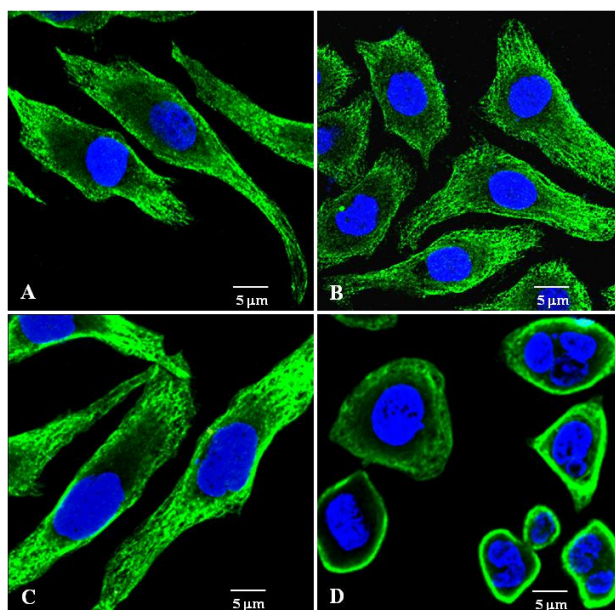


Figure 6. Effect of PXL on microtubule stabilization after survivin down-regulation in SKOV3-tr cells. SKOV3-tr cells were pre-treated with 200 nM survivin siRNA PM for 48 h followed by the treatment with 40 nM of PXL for 24 h. Cells were then stained for β -tubulin (green). The nuclei (blue) were stained with DAPI. A-D: Representative images of three independent experiments showing organization of microtubules. Untreated cells (A); cells treated with free PXL for 24h (B); cells treated with survivin siRNA PM for 72 h (C); cells pre-treated with survivin siRNA PM for 48 h followed by treatment with PXL for 24 h (D). Data = mean \pm SD (n =3).

Multifunctional therapy: survivin siRNA-S-S-PE and PXL co-encapsulated in PM

Finally, we investigated the effect of survivin siRNA-S-S-PE and PXL co-loaded in PM on the viability of a PXL-resistant cancer cell line, SKOV3-tr. For this purpose, we studied the effect of increasing concentrations of survivin siRNA-S-S-PE and PXL co-encapsulated in PM on the cell viability. In Figure 7, the viability of SKOV3-tr cells (%) 72 h after the treatment with free PXL, survivin siRNA PM and survivin siRNA/PXL PM, is shown. After the treatment with free PXL, no significant inhibition of the cell growth was observed. On the contrary, the simultaneous delivery of PXL and survivin siRNA-S-S-PE by PM to SKOV3-tr cells lead to a

significant inhibition of cell growth compared to all other treatments ($p < 0.001$ survivin siRNA/PXL PM *versus* the other treatments).

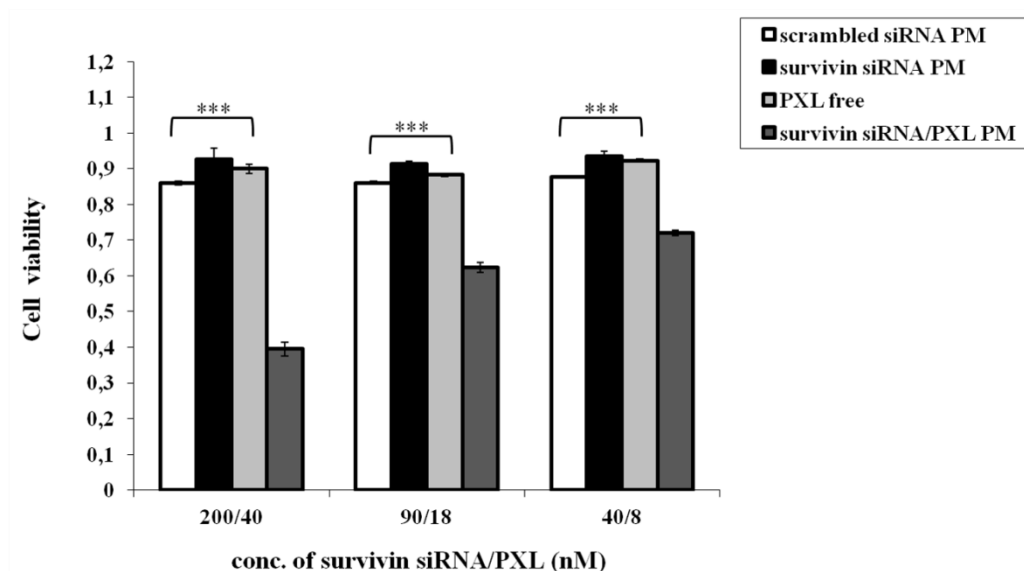


Figure 7. The viability of SKOV3-tr cancer cells. The cells were treated with the different formulations at 37°C for 6 h. After 72 h, the cell viability was measured by the Cell Titer Blue assay. Data = mean \pm SD (n = 3). *** $p < 0.001$ values were obtained by comparing each treatment to survivin siRNA/PXL PM treated cells.

Therapeutic efficacy of survivin siRNA/PXL PM on an animal model of PXL resistant ovarian cancer, SKOV3-tr.

Since in SKOV3-tr cell lines, the simultaneous delivery of PXL and survivin siRNA by using PM strengthens significantly the cytotoxicity induced by free or micellar PXL, the antitumor efficiency of such combination was investigated in an animal model of SKOV3-tr xenografts. To this purpose immune-suppressed mice were injected with SKOV3-tr cells and starting from day 15 treated with Taxol, scrambled siRNA/PXL PM, survivin siRNA PM and survivin siRNA/PXL PM once a week for five consecutive weeks. The anti-tumor efficacy was assessed by evaluation of the relative tumor volume (RTV) during therapy and the post-

mortem tumor weights. As reported in Figure 8A, PXL by itself, both in Cremophore solution (Taxol) and incorporated in PM (scrambled siRNA/PXL PM), did not induced a significant effect in the tumor growth. On the contrary, following the treatment of the animals with PM containing survivin siRNA alone or in combination with PXL the therapeutic outcome changed dramatically. Surprisingly, on the contrary to what observed previously *in vitro* in SKOV3-tr cell lines (Salzano G. *et al.*, 2014), the treatment with survivin siRNA alone was able to induced a significant slowing of the tumor growth. This effect was even more pronounced in survivin siRNA/PXL PM treated group. In particular, the treatment of mice with the combination elicited a marked antitumor activity, showing the least RTV among all the treatment groups ($P < 0.05$). Moreover, the tumor weights of mice treated with this schedule, evaluated after sacrifice the animals, was significantly reduced compared to all the control groups ($P < 0.01$) (Figure 8B). None of the agents caused any over toxicity, we did not detect significant changes in body weight (Figure 8C), toxic adverse events or deaths, confirming low non-specific toxicity of the treatments. To monitor the general toxicity after repeated doses of the treatments, the serum levels of ALT and AST were measured. As reported in Table III, there was no significant decrease of ALT and AST levels in serum following all the treatment groups, suggesting the absence of liver toxicity induced by the treatments.

Treatments	AST (IU/L)	ALT (IU/L)
PBS	10.44 ± 0.14	24.33 ± 0.13
Taxol	9.37 ± 0.34	18.17 ± 0.13
Scrambled siRNA/PXL PM	10.17 ± 0.18	19.64 ± 0.29
Survivin siRNA PM	11.21 ± 0.06	19.01 ± 0.08
Survivin siRNA/PXL PM	9.94 ± 0.52	18.27 ± 0.31

Table III. Evaluation of repeated dosing toxicity in mice by measurement of changes in serum levels of transaminase (AST/ALT).

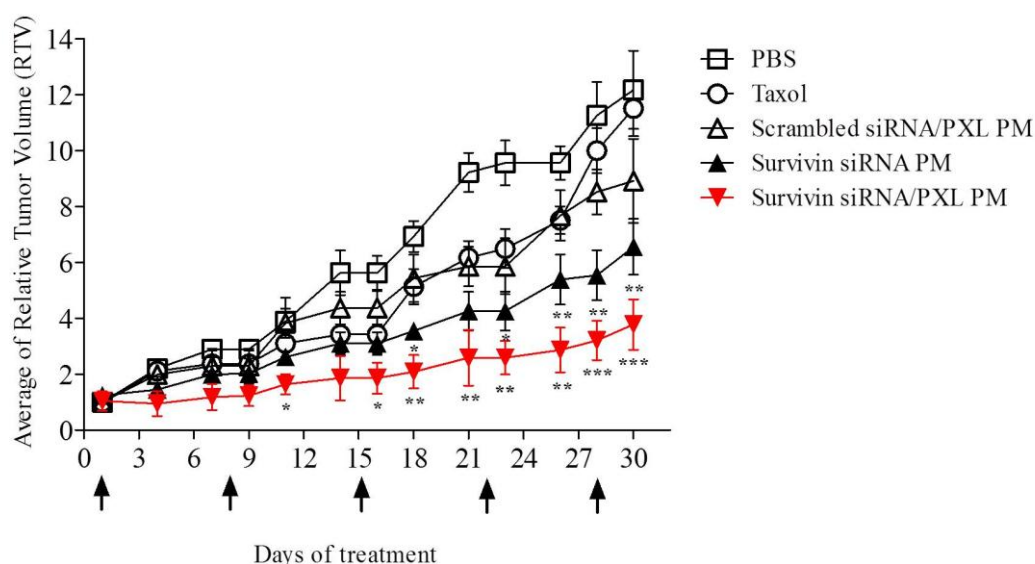


Figure 8 A. In vivo antitumor activity of survivin siRNA/PXL PM in SKOV3-tr xenografts. Survivin siRNA/PXL PM were administered at a final concentration of anti-survivin siRNA and PXL of 1 and 10 mg/kg, respectively, once per week for 5 consecutive weeks. Relative tumor volume (RTV) values (Tumor volume in mm³ on day 'n' (V_n) / tumor volume at the start of the treatment (V₀) plotted versus time in days) are reported. Data were given as mean ± SD for each treatment group. *p < 0.05, **p < 0.01, and ***p < 0.005 were obtained by comparing each treatment group with Taxol group.

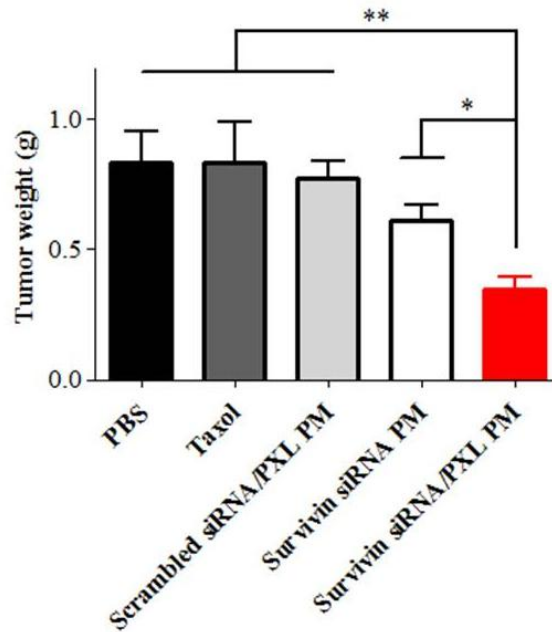


Figure 8 B. Post-mortem tumor weights. On day 30, heterotopically implanted tumors were weighed and plotted. * $p < 0.05$ and ** $p < 0.01$ were considered significant and very significant, respectively, and were obtained by comparing each treatment group with survivin siRNA/PXL group.

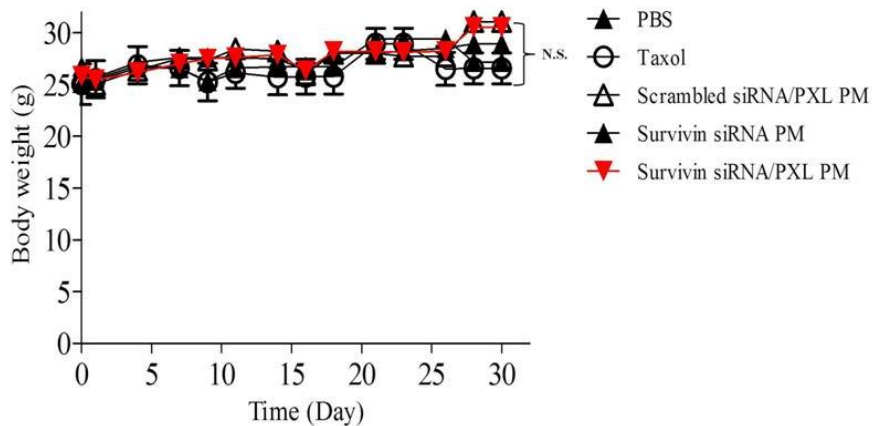


Figure 8C. Body weight of nude mice bearing SKOV3-tr measured every 3 days during the study. P values were considered no significant (N.S.) and were obtained by comparing each treatment group with survivin siRNA/PXL group.

Tumor tissues apoptosis

In order to investigate the biochemical mechanisms on the basis of the inhibition of the tumor growth in mice treated with survivin siRNA/PXL PM, the apoptotic effect was evaluated. Tumor sections of tumors dissected from the previous experiment were stained by Hoechst 33342, and apoptosis was analyzed by TUNEL assay under confocal microscopy. As shown in Figure 9, the co-delivery of PXL and survivin siRNA leads to the highest rate of cell apoptosis (Figure 9E), which was clearly superior to all the other treatment groups.

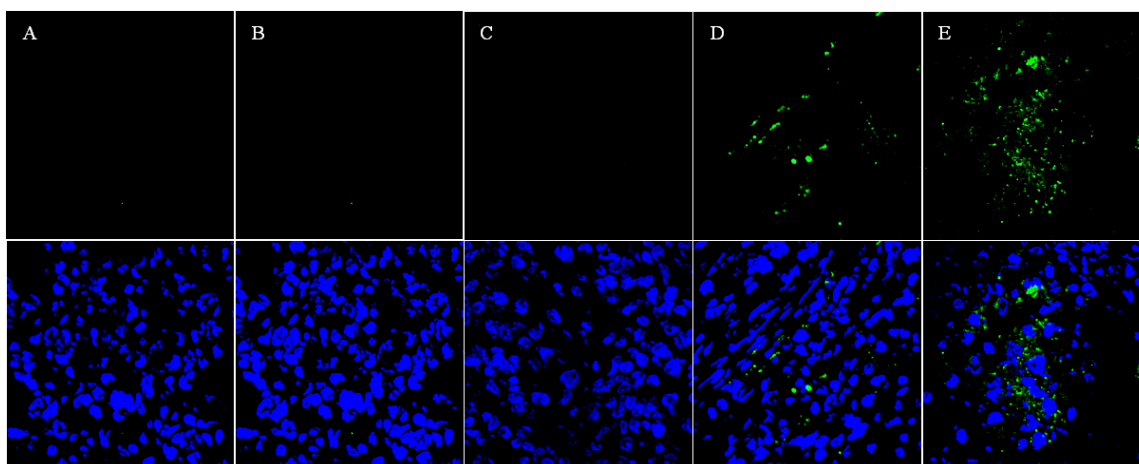


Figure 9. Apoptosis analysis on tumor sections by TUNEL assay. Pictures were taken by confocal microscopy (40x magnification). The nuclei were stained for Hoechst and apoptotic cells (green) for TUNEL. Representative images of (A) Untreated, (B) Scrambled siRNA/PXL PM, (C) Taxol, (D) Survivin siRNA PM, (E) Survivin siRNA/PXL PM groups.

Down-regulation of survivin mRNA expression *in vivo*

To provide evidence that the inhibition of the tumor growth by using survivin siRNA/PXL PM was due to its ability to down-regulate survivin *in vivo*, transcriptional mRNA of survivin gene expression was evaluated in tumor tissues by RT-PCR. Experiments were repeated three times. The

relative levels of survivin mRNA in tumor tissues were normalized against mRNA of an internal control gene, β -actin, performed in the same run (Wang Z. *et al.*, 2005). As shown in Figure 10, the relative levels of survivin mRNA in mice treated with survivin siRNA/PXL PM (0.09 ± 0.03) was significantly decreased compared with untreated (0.99 ± 0.007) and scrambled siRNA/PXL PM (0.86 ± 0.05) animal groups. The co-delivery of anti-survivin siRNA and PXL showed an inhibitory rate of survivin mRNA of about 90%. Interestingly, the treatment with Taxol could also reduce the survivin expression in tumors (Figure 10). In accordance with those previously reported by Hu Q. *et al.*, (2012), PXL free, as a result of mitosis inhibition, reduced temporarily the expression of survivin. These results indicated that the combination of an anti-survivin siRNA with a chemotherapeutic agent, such as PXL, with effective silencing propriety on survivin expression, could be a powerful approach to treat MDR tumors.

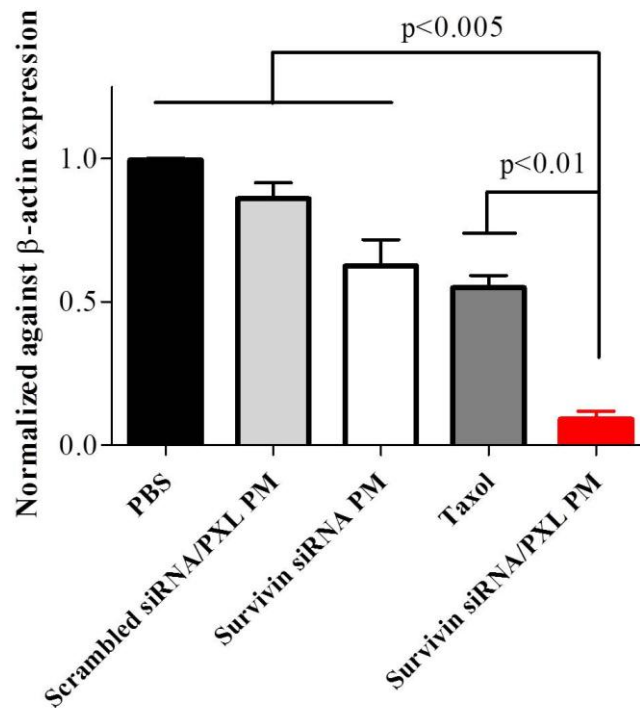


Figure 10. Survivin mRNA levels in tumor tissues by rt-PCR analysis. Data were given as mean \pm SD for each treatment group. ** $p < 0.01$, *** $p < 0.005$ were obtained by comparing each treatment group with survivin siRNA/PXL group.

Espression of survivin protein detected by immunofluorescence analysis

In order to confirm the data obtained by RT-PCR analysis, protein levels of survivin in tumor xenografts were investigated by immunohistochemical analysis. As shown in Figure 11A, the microscopic examination of stained tumor sections showed strong immunoreactivity for survivin (red color) in untreated and scrambled siRNA/PXL PM groups. In contrast, the intensity of survivin signal was dramatically decreased in survivin siRNA PM and survivin siRNA/PXL PM treated groups. Furthermore, the simultaneous delivery of PXL and gene in tumors was examined by confocal laser scanning microscope. For confocal microscopy observation, immunostaining for survivin, as described above, was used to evaluate the gene silencing and Oregon Green labeled PXL was used to follow the drug.

In particular, mice were treated once with survivin siRNA/PXL PM. After 48 hours the animals were injected with survivin siRNA/PXL PM containing Oregon Green labeled PXL. One hour later, the animals were sacrificed and tumors sections were processed under light protection. The confocal microscopy study showed clearly that Oregon Green labeled PXL was transported in the tumor tissues and survivin was significant down-regulated (Figure 11B). It is interesting to note that, a single administration of survivin siRNA/PXL PM was able to efficiently down-regulate survivin expression in tumors, as suggested by the almost absence of the survivin red signal in the sections.

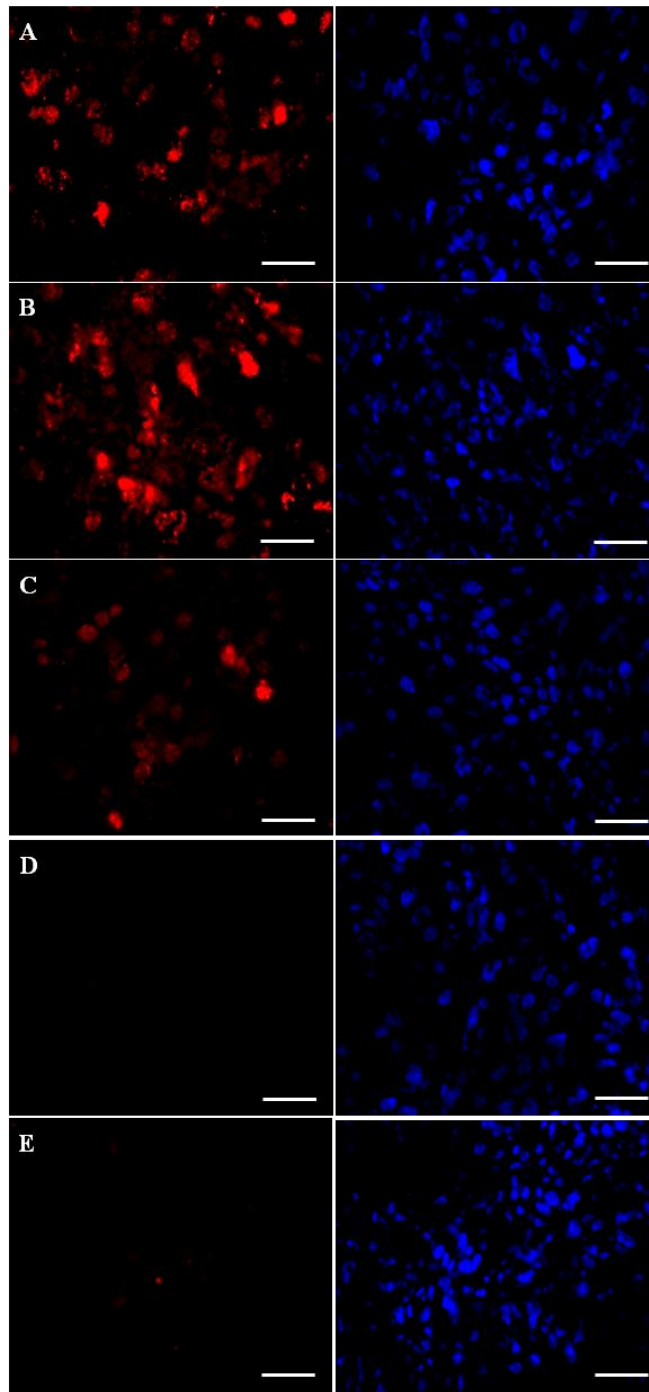


Figure 11 A. Immunohistochemistry analysis: Survivin protein levels was evaluated by fluorescent microscope (50 x). Representative images of three independent experiments showing survivin expression (in red). Untreated group (A); Scrambled siRNA/PXL PM group (B); Taxol group (C); Survivin siRNA PM group (D); Survivin siRNA/PXL PM group (E). Scale bar 5 μ m.

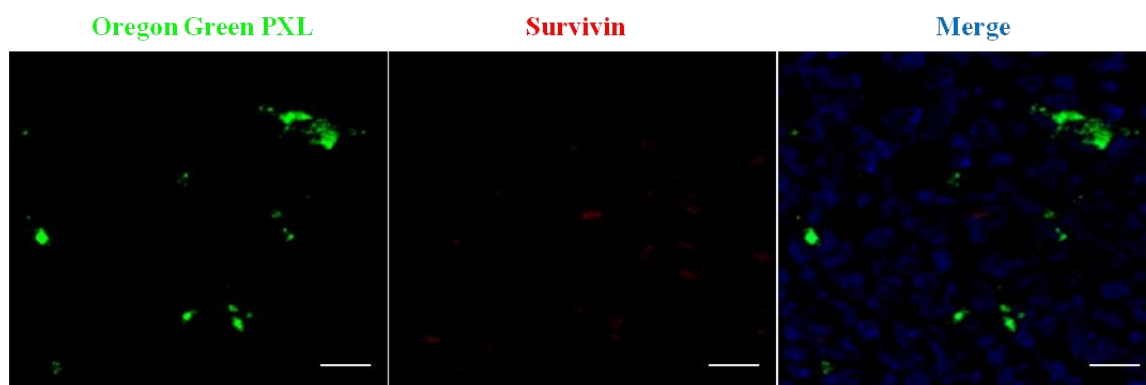


Figure 11 B. Simultaneous down-regulation of survivin expression and PXL penetration in tumor tissues by using survivin siRNA/PXL PM (63x). At the same time, the intra-tumor accumulation of Oregon Green labeled PXL (*left*) and survivin protein expression (*middle*) were evaluated on tumor sections by confocal microscopy (magnification 63x). Scale bar 5 μ m.

Effect of survivin siRNA/PXL PM on microtubule conformation of ovarian cancer xenografts

Previously, we have shown that survivin down-regulation enhanced the PXL activity on microtubule organization in SKOV3-tr cells. In particular, after down-regulation of survivin levels by treating cells with survivin siRNA PM, PXL was able to destabilize the microtubule organization at a very low concentration and exposition time. Here, to assess the effect of survivin siRNA/PXL PM on microtubule organization in vivo, SKOV3-tr tumor sections were incubated with an anti-tubulin fluorescent antibody. As shown in Figure 12A, in untreated mice, tumor cells exhibited staining of elongated microtubule fibers, demonstrative of an intact microtubule network. No significant difference were observed in all the other control groups (Figure 12 B-C-D). Interestingly, survivin siRNA/PXL PM group showed a microtubule-staining organization that was markedly different from all the other treatments (Figure 12E). In particular, as indicated by the arrows, in survivin siRNA/PXL PM treated mice, the tumor cells exhibited

diffuse and separate dense organization of microtubules in all the tissue (Figure 12 E). This results can be demonstrative of a no intact microtubule network.

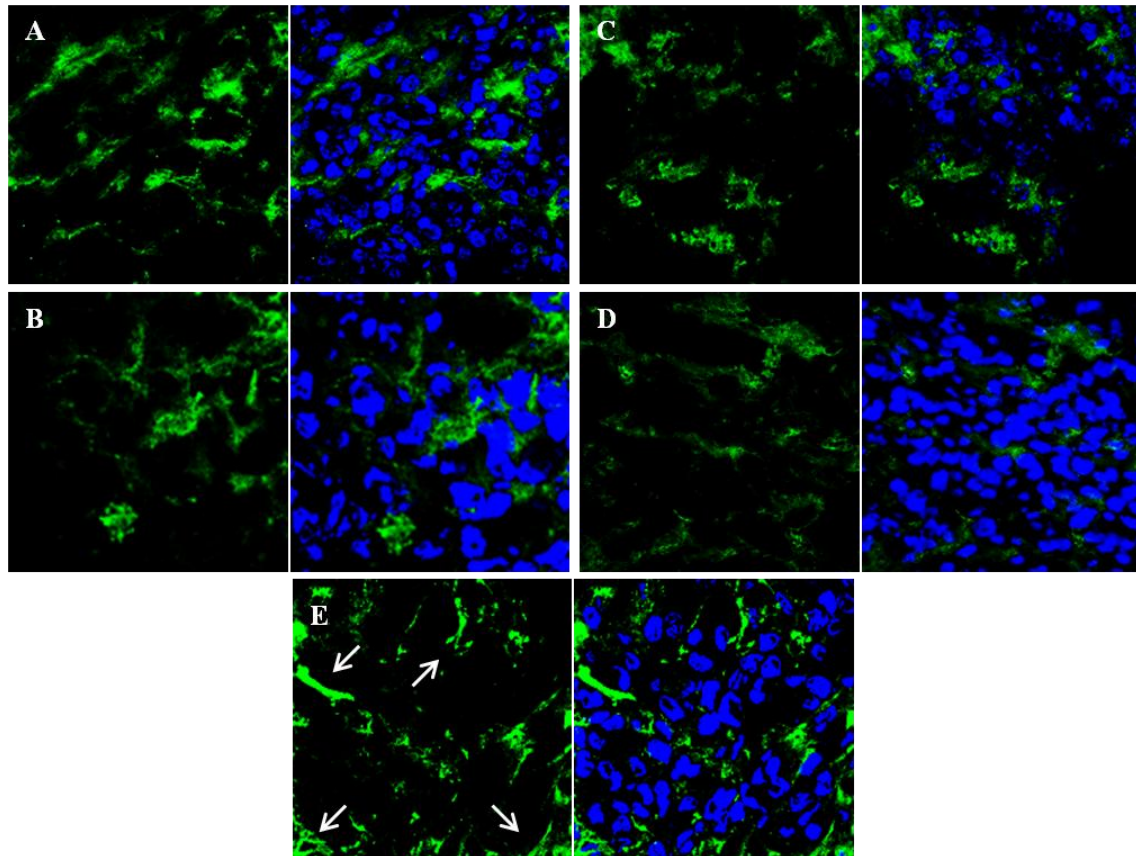


Figure 12. Microtubule organization after treatment with survivin siRNA/PXL PM *in vivo*. SKOV3-tr tumor sections were stained for β -tubulin (green). The nuclei (blue) were stained with Hoechst. A-E: Representative images of three independent experiments showing organization of microtubules. Untreated group (A); scrambled siRNA/PXL PM group (B); Taxol group C); survivin siRNA PM group (D); survivin siRNA/PXL PM group (E). Data = mean \pm SD (n =3).

Discussion

Survivin, a member of the IAP family, is considered a challenging target for cancer therapy. Survivin, not usually detected in normal adult tissue, is over-expressed in malignant tumors where plays a key role in hampering apoptosis, promoting cell proliferation, mitosis and angiogenesis (Altieri D.C. *et al.*, 2008). Moreover, there is evidence that survivin up-regulation may be a predictive factor in determining drug-resistance. Interestingly, it has been demonstrated that survivin inhibition reduces tumor growth potential and markedly enhances tumor cell response to anticancer agents, such as PXL, etoposide, cisplatin (Zaffaroni N. *et al.*, 2002), as well as to immunotherapy and ionizing radiation (Kanwar J.R. *et al.* 2001, Sah N.K. *et al.*, 2006). The resounding demonstrations of the efficacy of survivin inhibition in pre-clinical experiments has strongly incited to develop new strategies to target survivin in human tumors. Recently, siRNA directed against survivin, has been proposed as valid approach to specifically suppress survivin in cancer cells. In fact, it was shown to sensitize and strengthen the tumor response to chemotherapeutic drugs (Shapira A. *et al.*, 2011). However, the major obstacle to therapeutic RNAi is the disadvantageous biopharmaceutical profile, which strongly hampers achieving effective concentrations in intracellular site of action. Therefore, delivery strategies that stabilize siRNA and enhance intracellular uptake *in vivo* need to be developed.

A new method addressed to stabilize and deliver the siRNA was recently proposed by Prof. Torchilin V.P. group. In particular, a siRNA “reversibly” conjugated to a phospholipid by a disulfide linkage was synthesized (Musacchio T. *et al.*, 2010). The resulting modified siRNA was

incorporated in nanosized PEG₂₀₀₀-PE PM via its hydrophobic lipid moiety. As a result, the stability of PM-incorporated siRNA against nucleolytic degradation was dramatically increased, and, at the same time, the system easily released free unmodified siRNA in reducing conditions (similar to those inside cancer cells with characteristic high glutathione concentration). PEG₂₀₀₀-PE micelles has gained in the last years much attention due to their high stability *in vivo*, the possibility to efficiently encapsulate poor soluble drugs, such as PXL (Sawant R.R. *et al.*, 2010), and the ability to be accumulate in tumors via the EPR effect. In the present work, a siRNA against survivin was modified with a PE moiety and then incorporated in nanosized PM in order to deliver the survivin siRNA in cancer cells.

The survivin siRNA-S-S-PE was synthesized with a 90% of reaction yield. PM containing survivin siRNA optimized in terms of polymer concentration and weight ratio between polymer and survivin siRNA-S-S-PE demonstrated a mean size of about 20 nm and a narrow size distribution. The survivin siRNA was efficiently incorporated in PM only when a higher amount of PEG₂₀₀₀-PE was used. In particular, the use of a survivin siRNA/PEG₂₀₀₀-PE weight ratio of 1:750 allowed reaching the encapsulation efficiency of about 50% (Figure 2). The hydrophobic interaction between the PE moiety of siRNA-S-S-PE and that of the PEGylated lipid serves as the driving force underlying lipid-modified siRNA firm incorporation into PM.

Cell culture experiments showed a significant cytotoxic effect of survivin siRNA when delivered by PM. In particular, the treatment with survivin siRNA PM resulted in a significant decrease in cell viability in sensitive cancer cells and a significant down-regulation of survivin protein

levels, which was well in line with some previous observations (Li S.D. *et al.*, 2006). It is noteworthy that in a resistant cancer cell line (SKOV3-tr), although little cytotoxic effect was observed, a significant down-regulation of survivin was still achieved following treatment with survivin siRNA PM. In all the cases, the treatment with the scrambled siRNA conjugate in PM and plain PM did not yield any noticeable effect (Figures 3 and 4). Thus, PM proposed in this study are able to deliver the anti-survivin siRNA into the cells, as demonstrated by the significant inhibition of survivin expression. It is important that survivin siRNA PM demonstrated a silencing activity even in presence of serum. Free siRNA or siRNA delivered by commercial transfection agents, such as Lipofectamine, has no activity in presence of serum (Whitehead K.A. *et al.*, 2009). Evidently, the PEG shell layer of PM sterically shields the siRNA in PM from accessibility of serum proteins, thereby protecting it from aggregation and enzymatic degradation.

As the next step, we have investigated the potential of combination therapy with anti-survivin siRNA and a chemotherapeutic agent, PXL. PXL, one of the broad spectrum anticancer agents, was selected as a model anticancer drug, due to its efficacy often hampered by acquiring drug resistance by cancer cells (Podolski-Renić A. *et al.*, 2011). On the other hand, there are different lines of evidence indicating that survivin inhibition enhances the antitumor activity of PXL (Shen J. *et al.*, 2013; Hu Q. *et al.*, 2012). With this in mind, we investigated the potential of the survivin down-regulation by survivin siRNA PM on the chemosensitization of cancer cells to PXL. With this in mind, we have studied the effect of cell pre-treatment survivin siRNA on the PXL chemosensitization of sensitive

and resistant cancer cells. In sensitive cancer cells (MDA-MB231 and SKOV3), the pre-treatment with survivin siRNA for 48 h before exposing the cells to PXL, elicited a significant improvement in the cytotoxicity of the drug. In particular, a significant cytotoxic effect of PXL was observed at earlier times, namely after only 24 h of PXL treatment. In the same condition, but without the pre-treatment with survivin siRNA PM, PXL showed a cytotoxic effect only after 72 h of treatment. It is noteworthy that in the human paclitaxel-resistant cancer cells, SKOV3-tr, even after 72 h no any significant cytotoxicity was observed following treatment with PXL alone. The pre-treatment of SKOV3-tr with survivin siRNA PM and the consequent survivin down-regulation lead to a significant cell sensitization to PXL (Figure 5).

To confirm the key role of the survivin down-regulation on PXL sensitization in SKOV3-tr cell line, we have studied the microtubules organization by immunostaining the cells treated for β -tubulin. Survivin has been shown to bind polymerized microtubules *in vitro* where, presumably, it stabilizes the mitotic spindle (Li F. *et al.*, 1998). Tran J. *et al.* (2002) demonstrated a role of survivin in maintaining the integrity of the microtubule network of a human endothelial cell (HUVECs). In particular, they showed that in HUVECs cells, retrovirally infected with wild-type survivin, the over-expression of survivin could preserve the microtubule integrity of the cells treated with PXL. Our results suggest that survivin siRNA PM mediated survivin down regulation and could counteract the PXL chemoresistance in SKOV3-tr cell lines (Figure 6). In fact, in the absence of the pre-treatment with survivin siRNA PM, no changes on the microtubules morphology were observed after exposure to

PXL. The microtubules appeared like in “healthy” cells, with elongated and spread out tubulin filaments. Interestingly, in survivin siRNA PM pre-treated cells, the exposure to only 40 nM of PXL for 24 h, yielded significant changes in microtubules morphology. In particular, SKOV3-tr cells displayed a significant lack of microtubule organization reflective of cell death. Our data, therefore, support previous works demonstrating that survivin over-expression can negatively influence the sensitivity of cancer cell lines to chemotherapeutic agents, such as PXL.

In a last phase of the project, we have investigated if the developed PM could be used for co-encapsulation of survivin siRNA and PXL in mixed PM, in order to deliver simultaneously the two agents in cancer cells. With this in mind, we have evaluated if the presence of PXL could affect the properties of survivin siRNA PM in terms of size distribution and survivin siRNA encapsulation efficiency. When PXL was added to survivin siRNA PM, no changes in the size and in the encapsulation efficiency was observed. The mixed PM co-loading the two agents demonstrated a narrow size distribution and an incorporation efficiency of survivin siRNA and PXL of about 50% and 70%, respectively. Then, we investigated the *in vitro* and then, *in vivo* activity of the multifunctional PM in a PXL-resistant ovarian cancer, SKOV3-tr. The *in vitro* results revealed that the simultaneous delivery of PXL and survivin siRNA in the cells lead to a significantly enhanced cytotoxicity (Figure 7). In particular, after 72 h of treatment with PM containing the two agents combined, a strong cytotoxic effect was observed. On the contrary, the treatment with free PXL did not elicit any significant effect. In accordance with previous findings (Shen J. *et al.*, 2012) and the data observed by immunohistochemical analysis,

survivin inhibition can strongly influence the sensitivity of SKOV3-tr cells to PXL.

Finally, the anti-tumor effect of anti-survivin siRNA and PXL co-loaded in PM was demonstrated in nude mice bearing SKOV3-tr tumors. The animals were treated with Taxol, scrambled siRNA/PXL PM, survivin siRNA PM and survivin siRNA/PXL PM once a week for five consecutive weeks at doses of 1 and 10mg/kg for PXL and siRNA, respectively. During the treatment, the overall health of the animals was good. No weight loss or evident hepatotoxicity was found after repeated doses of the different PM formulations or even Taxol (Table III). It is worth noticing that intravenous injections of Taxol (PXL~ 10 mg/kg) twice a week produced significant body loss in SKOV-3 xenografted mice with poor improvement in the therapeutic outcome.

Combination of PXL and survivin siRNA in PM resulted in sensitization of resistant tumors to PXL and improved anti-cancer activity. As shown in Figure 8A, the co-delivery of anti-survivin siRNA and PXL in PM inhibited tumor growth and exceeded the therapeutic effect of single agents. Mice treated with survivin-siRNA/PXL PM showed a 4-fold tumor volume reduction as compared to saline control that consistent with the half-reduction in tumor weight after the sacrifice of the animals. Survivin down-regulation by survivin siRNA PM exhibited certain anti-cancer activity although lesser than observed in animal treated with survivin siRNA/PXL-PM. This intrinsic anti-cancer activity was already described in SKOV3 animal model by direct tumor injection of survivin shRNA (Xing J. *et al.*, 2012). Finally, the lack of therapeutic response of PXL either as Taxol or incorporated into scrambled siRNA/PXL PM

demonstrated that survivin down-regulation mediated the sensitization of resistant tumors to non-effective doses of PXL.

Sequence-specific down-regulation by survivin siRNA in PM was confirmed in excised tumors (Figure 10). Taxol-treated tumors had significant decreased levels of survivin mRNA as previously described (Wang Z. *et al.*, 2005) whereas protein levels were not significantly decreased. Only those nanopreparations containing anti-survivin siRNA were able to consistently decrease survivin mRNA and protein levels at the same extent.

We further characterized the tumor response to survivin siRNA and PXL combination by the detection of apoptosis in tumor sections. The degree of apoptosis (Figure 9) correlated well with the tumor growth curves. The highest level of tumor apoptosis was found for survivin siRNA/PXL PM followed by survivin siRNA PM, whereas no significant apoptosis increase was found for PXL formulations (Figure 9). Finally, the restoration of PXL sensitivity by survivin siRNA/PXL PM treatment was also noticed by the changes in the microtubule network in tubulin-stained tumor sections (Figure 12). Similar to what we observed *in vitro* (Salzano G. *et al.*, 2014), survivin siRNA/PXL PM treatment resulted in more intensively stained tubulin as compared with the rest of the preparations, consistent with an improvement of the micro-tubule-stabilizing activity of PXL (Anbalagan M. *et al.*, 2012).

Conclusions

We have developed a micellar nanopreparation (PM) containing anti-survivin siRNA as siRNA-S-S-PE conjugate and PXL for the treatment of ovarian cancer. The developed system allows for easy and highly efficient co-encapsulation of chemotherapeutic drugs and siRNA, showed high colloidal stability and small particle sizes compatible with parenteral administration and tumor targeting. The micelles accumulate in distal tumors and delivered anti-survivin siRNA and PXL in sufficiently high amounts to mediate a potent and specific survivin down-regulation and improved anti-cancer activity as compared to single agents. Survivin down-regulation by anti-survivin siRNA/PXL PM mediated the sensitization of the resistant ovarian tumor to non-effective doses of PXL. Finally, the system avoids the use of toxic excipients and is well-tolerated by the animals even after repeated dosing. On the whole, these results demonstrated that the survivin siRNA-S-S-PE PM developed in this work look like a promising tool to inhibit survivin expression in cancer cells. Moreover, due to the possibility to co-encapsulate lipophilic drugs, such as PXL, this system could be also used to overcome multidrug resistance in the treatment of chemoresistant tumors.

References

Addeo R., De Santi M.S., Del Prete S., Caraglia M. Fotemustine and recurrent glioblastoma: possible new opportunities for an old drug. *Cancer Chemother Pharmacol.* 2009;64:863-6.

Altieri D.C. Survivin, cancer networks and pathway-directed drug discovery. *Nat. Rev Cancer.* 2008;8:61-70.

Altieri D.C. Validating survivin as a cancer therapeutic target. *Nat. Rev. Cancer.* 2003;3:46-54.

Ambrosini G., Adida C., Altieri D.C. A novel anti-apoptosis gene, survivin, expressed in cancer and lymphoma. *Nat. Med.* 1997;3:917-21.

Anbalagan M., Ali A., Jones R.K., Marsden C.G., Sheng M., Carrier L., *et al.* Peptidomimetic Src/pre-tubulin inhibitor KX-01 alone and in combination with paclitaxel suppresses growth, metastasis in human ER/PR/HER2-negative tumor xenografts. *Mol Cancer Ther.* 2012;11(9):1936-47.

Aparicio A., Gardner A., Tu Y., Savage A., Berenson J., Lichtenstein A.. *In vitro* cytoreductive effects on multiple myeloma cells induced by bisphosphonates. *Leukemia.* 1998;12:220-9.

ASTM F-756. Standard Practice for Assessment of Hemolytic Properties of Materials. *Annual Book of ASTM Standards.* 2009.

Balendiran G.K., Dabur R., Fraser D. The role of glutathione in cancer. *Cell Biochem. Funct.* 2004;22:343–52.

Burdo J.R., Antonetti D.A., Wolpert E.B., Connor J.R. Mechanisms and regulation of transferrin and iron transport in a model blood-brain barrier system. *Neuroscience*. 2003;121:883-90.

Caplen N.J., Parrish S., Imani F., Fire A., Morgan R. A. Specific inhibition of gene expression by small doublestranded RNAs in invertebrate and vertebrate systems. *Proc. Natl. Acad. Sci. U.S.A.* 2001;98:9742-7.

Caraglia M., D'Alessandro A.M., Marra M., Giuberti G., Vitale G., Viscomi C., Colao A., Prete S.D., Tagliaferri P., Tassone P., Budillon A., Venuta S., Abbruzzese A. The farnesyl transferase inhibitor R115777 (Zarnestra) synergistically enhances growth inhibition and apoptosis induced on epidermoid cancer cells by Zoledronic acid (Zometa) and Pamidronate. *Oncogene*. 2004;23:6900-6913.

Caraglia M., Santini D., Marra M., Vincenzi B., Tonini G., Budillon A. Emerging anti-cancer molecular mechanisms of aminobisphosphonates. *Endocr. Relat. Cancer*. 2006;13:7-26.

Carvalho A., Carmena M., Sambade C., Earnshaw W.C., Wheatley S.P., Survivin is required for stable checkpoint activation in taxol-treated HeLa cells. *J. Cell Sci*. 2003;116:2987-98.

Chaturvedi K. *et al.* Cyclodextrin-based siRNA delivery nanocarriers: a state-of-the-art review. *Expert Opin Drug Deliv*. 2011.

Chen C., Cheng Y.C., Yu C.H., Chan S.W., Cheung M.K., Yu P.H. *In vitro* cytotoxicity, hemolysis assay, and biodegradation behavior of biodegradable poly(3-hydroxybutyrate)-poly(ethylene glycol)-poly(3-

hydroxybutyrate) nanoparticles as potential drug carriers. *J Biomed Mater Res A*.2008;87:290-8.

Chen T., Berenson J., Vescio R., Swift R., Glichick A., Goodin S., LoRusso P., Ma P., Ravera C., Deckert F., Schran H., Seaman J & Skerjanec A. Pharmacokinetics and pharmacodynamics of zoledronic acid in cancer patients with bone metastases. *J Clin Pharmacol*. 2002;42:1228–1236.

Chinot O.L., Macdonald D.R., Abrey L.E., Zahlmann G., Kerloëguen Y., Cloughesy T.F. Response assessment criteria for glioblastoma: practical adaptation and implementation in clinical trials of antiangiogenic therapy. *Curr Neurol Neurosci Rep*. 2013;13:347.

Chu T.C., Twu K.Y., Ellington A.D., Levy M. Aptamer mediated siRNA delivery. *Nucleic Acids Res*. 2006; 34, e73.

Crommelin D.J., Florence A.T. Towards more effective advanced drug delivery systems. *Int J Pharm*. 2013;454(1):496-511.

Daniels T.R., Bernabeu E., Rodríguez J.A., *et al*. The transferrin receptor and the targeted delivery of therapeutic agents against cancer. *Biochim Biophys Acta*. 2012;1820:291-317.

Davis M.E. The first targeted delivery of siRNA in humans via a self-assembling, cyclodextrin polymer-based nanoparticle: from concept to clinic. *Mol. Pharm*. 2009.

De Rosa G., Caraglia M. New Therapeutic Opportunities from Old Drugs: The Role of Nanotechnology? Editorial. *Journal of Bioequivalence & Bioavailability*. 2013.

Demeule M., *et al.* Expression of multi-drug resistant P-glicoprotein (MDR-1) in human brain tumors. *Int. J. Cancer.* 2001;93(1):62-6.

Doll T.A., *et al.* Nanoscale assemblies and their biomedical applications. *J R Soc Interface.* 2013.

Estrela J.M., Ortega A., Obrador E. Glutathione in cancer biology and therapy. *Crit. Rev. Clin. Lab. Sci.* 2006;43:143-81.

Facchini G., Caraglia M., Morabito A., Marra M., Piccirillo M.C., Bochicchio A.M., Striano S., Marra L., Nasti G., Ferrari E., Leopardo D., Vitale G., Gentilini D., Tortoriello A., Catalano A., Budillon A., Perrone F., Iaffaioli R.V. Metronomic administration of zoledronic acid and taxotere combination in castration resistant prostate cancer patients: phase I ZANTE trial. *Cancer Biology & Therapy.* 2010;10:543-548.

Fire A., Xu S., Montgomery M.K., S.A. Kostas, S.E. Driver, C.C. Mello, Potent and specific genetic interference by double-stranded RNA in *Caenorhabditis elegans.* *Nature.* 1998;391:806-11.

Gallagher B.M. Jr. Microtubule-stabilizing natural products as promising cancer therapeutics. *Curr. Med. Chem.* 2007;14:2959-67.

Gary-Bobo M., *et al.* Targeting multiplicity: the key factor for anti-cancer nanoparticles. *Curr Med Chem.* 2013;20(15):1946-55.

Grimm D., Streetz Jopling K. L., Storm C. L., Pandey T. A., Davis K., Marion C. R., Salazar P., Kay M. A. Fatality in mice due to oversaturation of cellular microRNA/ short hairpin RNA pathways. *Nature.* 2006;441: 537-41.

Hägerstrand H., Iglıc A., Bobrowska-Hägerstrand M., Lindqvist C., Isomaa B., Eber S. Amphiphile-induced vesiculation in aged hereditary spherocytosis erythrocytes indicates normal membrane stability properties under non-starving conditions. *Mol Membr Biol.* 2001;18:221-7.

Hannon G. J., Rossi J.J. Unlocking the potential of the human genome with RNA interference. *Nature.* 2004;431:371–8.

Hu Q., Li W., Hua X., Hua Q., Shen J., Jin X., Zhou J., Tang G., Chu P.K. Synergistic treatment of ovarian cancer by co-delivery of survivin shRNA and paclitaxel via supramolecular micellar assembly. *Biomaterials.* 2012; 33:6580-6591.

Jeong J.H. *et al.* Self-assembled and nanostructured siRNA delivery systems. *Pharm Res.* 2011.

Kainthan R.K., Gnanamani M., Ganguli M., Ghosh T., Brooks D.E., Maiti S., Kizhakkedathu J.N. Blood compatibility of novel water soluble hyperbranched polyglycerol-based multivalent cationic polymers and their interaction with DNA. *Biomaterials.* 2006;27:5377-90.

Kanwar J.R., Shen W.P., Kanwar R.K., Berg R.W., Krissansen G.W. Effects of survivin antagonists on growth of established tumors and B7-1 immunogene therapy. *J. Natl. Cancer Inst.* 2001;93:1541-52.

Kim S.H., Jeong J.H., Lee S.H., Kim S.W., Park T.G. PEG conjugated VEGF siRNA for anti-angiogenic gene therapy. *J. Controlled Release* 2006;116:123–9.

Kim S.H., Mok H., Jeong J. H., Kim S.W., Park T. G. Comparative evaluation of target-specific GFP gene silencing efficiencies for antisense

ODN, synthetic siRNA, and siRNA plasmid complexed with PEI-PEG-FOL conjugate. *Bioconjugate Chem.* 2006;17:241–4.

Korfel A., Thiel E.. Targeted therapy and blood-brain barrier. *Recent Results Cancer Res.* 2007;176:123-33.

Kurtzberg L.S., Roth S., Krumbholz R., Crawford J., Bormann C., Dunham S., Yao M., Rouleau C., Bagley R.G., Yu X.J., Wang F., Schmid S.M., Lavoie E.J., Teicher B.A. Genz-644282, a novel non-camptothecin topoisomerase I inhibitor for cancer treatment. *Clin Cancer Res* 2011;17:2777-87.

Lammers T. Tumour-targeted nanomedicines: principles and practice. *Br J Cancer.* 2008;99(3):392–7.

Landen C., Chavez-Reyes N. Jr., Bucana A., Schmandt C., Deavers R., Lopez-Berestein M.T., Sood G. Therapeutic EphA2 gene targeting in vivo using neutral liposomal small interfering RNA delivery. *Cancer Res.* 2005;65:6910–8.

Lee M.V., Fong E.M., Singer F.R., Guenette R.S. Bisphosphonate treatment inhibits the growth of prostate cancer cells. *Cancer Res* 2001;61:2602-8.

Li F., Ambrosini G., Chu E.Y., Plescia J., Tognin S., Marchisio P.C., Altieri D.C. Control of apoptosis and mitotic spindle checkpoint by survivin. *Nature.* 1998;396:580-4.

Li S.D., Huang L. Targeted Delivery of Antisense Oligodeoxynucleotide and Small Interference RNA into Lung Cancer Cells. *Mol. Pharm.* 2006;3: 579-588.

Liu S., Guo Y., Huang R., Li J., Huang S., Kuang Y. *et al.* Gene and doxorubicin co-delivery system for targeting therapy of glioma. *Biomaterials*. 2012; 33(19):4907-16.

LorenzHadwiger C., John P., Vornlocher M., Unverzagt H.P.C. Steroid and lipid conjugates of siRNAs to enhance cellular uptake and gene silencing in liver cells. *Bioorg. Med. Chem. Lett.* 2004;14:4975–7.

Lu J., Tan M., Huang W.C., Li P., Guo H., Tseng L.M., Su X.H., Yang W.T., Treekitkarnmongkol W., Andreeff M., Symmans F., Yu D. Mitotic deregulation by survivin in ErbB2-overexpressing breast cancer cells contributes to Taxol resistance *Clin. Cancer Res.* 2009;15:1326-34.

Marra M., Salzano G., Leonetti C., Porru M., Franco R., Zappavigna S., Liguori G., Botti G., Chieffi P., Lamberti M., Vitale G., Abbruzzese A., La Rotonda M.I., De Rosa G., Caraglia M. New self-assembly nanoparticles and stealth liposomes for the delivery of zoledronic acid: a comparative study. *Biotechnol. Adv.* 2012;30:302-9.

Marra M., Santini D., Meo G., Vincenzi B., Zappavigna S., Baldi A., Rosolowski M., Tonini G., Loeffler M., Lupu R., Addeo S.R., Abbruzzese A., Budillon A., Caraglia M. Cyr61 downmodulation potentiates the anticancer effects of zoledronic acid in androgen-independent prostate cancer cells. *Int J Cancer.* 2009;125:2004-13.

McManus M.T., Sharp P.A. Gene silencing in mammals by small interfering RNAs. *Nat. Rev. Genet.* 2002;3:737–47.

Mok H., Park T.G. Self-crosslinked and reducible fusogenic peptides for intracellular delivery of siRNA. *Biopolymers.* 2008.

Mokhtari K., Paris S., Aguirre-Cruz L., Privat N., Crinière E., Marie Y., Hauw J.J., Kujas M., Rowitch D., Hoang-Xuan K., Delattre J.Y., Sanson M. Olig2 expression, GFAP, p53 and 1p loss analysis contribute to glioma subclassification. *Neuropathol Appl Neurobiol.* 2005;31:62-9.

Moschos S. A., Jones S. W., Perry M.M., Williams A.E., Erjefalt J.S., Turner J.J., Barnes P.J., Sproat B.S., Gait M.J., Lindsay M.A. Lung delivery studies using siRNA conjugated to TAT(48-60) and penetratin reveal peptide induced reduction in gene expression and induction of innate immunity. *Bioconjugate Chem.* 2007;18:1450–9.

Muratovska A., and Eccles M. R. Conjugate for efficient delivery of short interfering RNA (siRNA) into mammalian cells. *FEBS Lett.* 2004;558:63–8.

Musacchio T., Laquintana V., Latrofa A., Trapani G., Torchilin V.P. PEG-PE micelles loaded with paclitaxel and surface-modified by a PBR-ligand: synergistic anticancer effect. *Mol. Pharm.* 2009;6:468-79.

Musacchio T., Vaze O., D'Souza G., Torchilin V.P. Effective Stabilization and Delivery of siRNA: Reversible siRNA-Phospholipid Conjugate in Nanosized Mixed Polymeric Micelles. *Bioconjugate Chem.* 2010;21:1530–1536.

Nardinocchi L., Pantisano V., Puca R., Porru M., Aiello A., Grasselli A., Leonetti C., Safran M., Rechavi G., Givol D., Farsetti A., D'Orazi G. Zinc downregulates HIF-1 α and inhibits its activity in tumor cells in vitro and in vivo. *PLoS One.* 2010.

Nishina K. , Unno T., Uno Y., Kubodera T., Kanouchi T., Mizusawa H., Yokota T. Efficient in vivo delivery of siRNA to the liver by conjugation of alpha-tocopherol. *Mol. Ther.* 2008;16:734–40.

Patel M.M., Goyal B.R., Bhadada S.V., Bhatt J.S., Amin A.F. Getting into the brain: approaches to enhance brain drug delivery. *CNS Drugs* 2009;23:35-58.

Pessina A., Albella B., Bayo M., Bueren J., Brantom P., Casati S., Croera C., Gagliardi G., Foti P., Parchment R., Parent-Massin D., Schoeters G., Sibiril Y., Van Den Heuvel R., Gribaldo L. Application of the CFU-GM assay to predict acute drug-induced neutropenia: an international blind trial to validate a prediction model for the maximum tolerated dose (MTD) of myelosuppressive xenobiotics. *Toxicol Sci.* 2003;75:355-67.

Podolski-Renić A., Anđelković T., Banković J., Tanić N., Ruždijić S., Pešić M. The role of paclitaxel in the development and treatment of multidrug resistant cancer cell lines. *Biomed. Pharmacother.* 2011;65:345-53.

Recht L., Torres C.O., Smith T.W., Raso V., Griffin T.W. Transferrin receptor in normal and neoplastic brain tissue: implications for brain-tumor immunotherapy. *J Neurosurg.* 1990;72:941–945.

Sah N.K., Munshi A., Hobbs M., Carter B.Z., Andreeff M., Meyn R.E. Effect of downregulation of survivin expression on radiosensitivity of human epidermoid carcinoma cells. *Int. J. Radiat. Oncol. Biol. Phys.* 2006;66:852-9.

Salzano G., Marra M., Porru M., Zappavigna S., Abbruzzese A., La Rotonda M.I., Leonetti C., Caraglia M., De Rosa G. Self-assembly nanoparticles for the delivery of bisphosphonates into tumors. *Int J Pharm* 2011;403:292-7.

Sampetrean O., Saya H. Characteristics of glioma stem cells. *Brain Tumor Pathol.* 2013;30:209-14.

Santel A., Aleku M., Keil O., Endruschat J., Esche V., Durieux B., Loffler K., Fechtner M., Rohl T., Fisch G., Dames S., Arnold W., Giese K., Klippel A., Kaufmann J. RNA interference in the mouse vascular endothelium by systemic administration of siRNA-lipoplexes for cancer therapy. *Gene Ther.* 2006;13:1360–70.

Sawant R.R., Torchilin V.P. Polymeric micelles: polyethylene glycol-phosphatidylethanolamine (PEG-PE)-based micelles as an example. *Methods Mol. Biol.* 2010;624:131-49.

Schafer W.R., Rine J. Protein prenylation: genes, enzymes, targets, and functions. *Annu Rev Genet.* 1992;26:209-237.

Senaratne S.G., Pirianov G., Mansi J.L., Arnett T.R., Colston K.W. Bisphosphonates induce apoptosis in human breast cancer cell lines. *Br J Cancer.* 2000;82:1459-68.

Seth S., Matsui Y., Fosnaugh K., Liu Y., *et al.* Polisky, RNAi-based therapeutics targeting survivin and PLK1 for treatment of bladder cancer. *Mol. Ther.* 2011;19:928-35.

Shapira A., Livney Y.D., Broxterman H.J., Assaraf Y.G. Nanomedicine for targeted cancer therapy: towards the overcoming of drug resistance. *Drug Resist. Updat.* 2011;14:150-63.

Shen J., Sun H., Xu P., Yin Q., Zhang Z., Wang S., Yu H., Li Y. Simultaneous inhibition of metastasis and growth of breast cancer by co-delivery of twist shRNA and paclitaxel using pluronic P85-PEI/TPGS complex nanoparticles. *Biomaterials.* 2013;34:1581-90.

Shen J., Yin Q., Chen L., Zhang Z., Li Y. Co-delivery of paclitaxel and survivin shRNA by pluronic P85-PEI/TPGS complex nanoparticles to overcome drug resistance in lung cancer. *Biomaterials.* 2012;33:8613-8624.

Singla A.K., Garg A., Aggarwal D. Paclitaxel and its formulations. *Int. J. Pharm.* 2002;235:179-92.

Skerjanec A., Berenson J., Hsu C., Major P., Miller W.H. Jr, Ravera C., Schran H., Seaman J., Waldmeier F. The pharmacokinetics and pharmacodynamics of zoledronic acid in cancer patients with varying degrees of renal function. *J Clin Pharmacol.* 2003;43:154–162.

Song E., Lee S.K., Wang J., Ince N., Ouyang N., Min J., Chen J., Shankar P., Lieberman J. RNA interference targeting Fas protects mice from fulminant hepatitis. *Nat. Med.* 2003;9:347–51.

Soutschek J., Akinc A., Bramlage B., Charisse K., Constien R., Donoghue M., Elbashir S., Geick A., Hadwiger P., Harborth J., John M., Kesavan V., Lavine G., Pandey R. K., Racie T., Rajeev K. G., Rohl I., Toudjarska I., Wang G., Wuschko S., Bumcrot D., Kotliansky V., Limmer S.,

Manoharan M., Vornlocher H.P. Therapeutic silencing of an endogenous gene by systemic administration of modified siRNAs. *Nature*. 2004;432: 173–8.

Torchilin V.P. Micellar nanocarriers: pharmaceutical perspectives. *Pharm Res*. 2007.

Torchilin V.P., Weissig V. Liposomes: A Practical Approach (2nd ed)Oxford Univ. Press, New York. 2003.

Tran J., Master Z., Yu J.L., Rak J., Dumont D.J., Kerbel R.S. A role for survivin in chemoresistance of endothelial cells mediated by VEGF. *Proc. Natl. Acad. Sci. U.S.A.* 2002;99:4349-54.

Urban-Klein B., Werth S., Abuharbeid S., Czubayko F., Aigner A. RNAi-mediated gene-targeting through systemic application of polyethylenimine (PEI)-complexed siRNA *in vivo*. *Gene Ther*. 2005;12:461–6.

Wang Z., Xie Y., Wang H. Changes in survivin messenger RNA level during chemotherapy treatment in ovarian cancer cells. *Cancer Biol Ther*. 2005;4(7):716-9.

Wang Z., Xie Y., Wang H. Changes in survivin messenger RNA level during chemotherapy treatment in ovarian cancer cells. *Cancer Biol Ther*. 2005;4(7):716-9.

Whitehead K.A., Langer R. Anderson D.G. Knocking down barriers: advances in siRNA delivery. *Nat. Rev. Drug Discov*. 2009;8:129–138.

Xing J., Jia C.R., Wang Y., Guo J., Cai Y. Effect of shRNA targeting survivin on ovarian cancer. *J Cancer Res Clin Oncol*. 2012;138(7):1221-9.

Xue X., Liang X.J. Overcoming drug efflux-based multidrug resistance in cancer with nanotechnology. *Chin J Cancer*. 2012;31(2):100-9.

Yadav S. *et al.* Evaluation of combination MDR-1 gene silencing and paclitaxel administration in biodegradable polymeric nanoparticles formulations to overcome multidrug resistance in cancer cells. *Cancer Chemother Pharmacol*. 2009; 63(4):711-22.

Yang D., Welm A., Bishop J.M. Cell division and cell survival in the absence of survivin. *Proc. Natl. Acad. Sci. U.S.A.* 2004;15100-5.

Yano J., Hirabayashi K., Nakagawa S., Yamaguchi T., Nogawa M., Kashimori I., Naito H., Kitagawa H., Ishiyama K., Ohgi T., Irimura T. Antitumor activity of small interfering RNA/cationic liposome complex in mouse models of cancer. *Clin. Cancer Res*. 2004;10:7721–6.

Zaffaroni N., Daidone M.G. Survivin expression and resistance to anticancer treatments: perspectives for new therapeutic interventions. *Drug Resist. Updat*. 2002;5:65-72.

Zhu J.J., Wong E.T. Personalized medicine for glioblastoma: current challenges and future opportunities. *Curr. Mol. Med*. 2013;13:358-67.

Zimmermann T.S., Lee A.C., Akinc A., *et al.* RNAi-mediated gene silencing in non-human primates. *Nature*. 2006;441:111–4.